13. Turner, M.D.; Nedjai, B.; Hurst, T.; Pennington, D.J. Cytokines and chemokines: At the crossroads of cell signalling and inflammatory disease. *Biochim. Biophys. Acta Mol. Cell Res.* **2014**, *1843*, 2563–2582. [CrossRef] [PubMed]
14. Günaltay, S.; Kumawat, A.K.; Nyhlin, N.; Bohr, J.; Tysk, C.; Hultgren, O.; Hultgren Hörnquist, E. Enhanced levels of chemokines and their receptors in the colon of microscopic colitis patients indicate mixed immune cell recruitment. *Mediat. Inflamm.* **2015**, *2015*, 132458. [CrossRef]
15. Kostova, Z.; Batsalova, T.; Moten, D.; Teneva, I.; Dzhambazov, B. Ragweed-allergic subjects have decreased serum levels of chemokines CCL2, CCL3, CCL4 and CCL5 out of the pollen season. *Cent. Eur. J. Immunol.* **2015**, *40*, 442–446. [CrossRef]
16. Aldinucci, D.; Colombatti, A. The inflammatory chemokine CCL5 and cancer progression. *Mediat. Inflamm.* **2014**, *2014*, 292376. [CrossRef]
17. Hughes, C.E.; Nibbs, R.J.B. A guide to chemokines and their receptors. *FEBS J.* **2018**, *285*, 2944–2971. [CrossRef]
18. Hong, S.N.; Joung, J.G.; Bae, J.S.; Lee, C.S.; Koo, J.S.; Park, S.J.; Im, J.P.; Kim, Y.S.; Kim, J.W.; Park, W.Y.; et al. RNA-seq Reveals Transcriptomic Differences in Inflamed and Noninflamed Intestinal Mucosa of Crohn's Disease Patients Compared with Normal Mucosa of Healthy Controls. *Inflamm. Bowel Dis.* **2017**, *23*, 1098–1108. [CrossRef]
19. Girbl, T.; Lenn, T.; Perez, L.; Rolas, L.; Barkaway, A.; Thiriot, A.; del Fresno, C.; Lynam, E.; Hub, E.; Thelen, M.; et al. Distinct Compartmentalization of the Chemokines CXCL1 and CXCL2 and the Atypical Receptor ACKR1 Determine Discrete Stages of Neutrophil Diapedesis. *Immunity* **2018**, *49*, 1062–1076. [CrossRef]
20. Zhou, G.X.; Liu, Z.J. Potential roles of neutrophils in regulating intestinal mucosal inflammation of inflammatory bowel disease. *J. Dig. Dis.* **2017**, *18*, 495–503. [CrossRef]
21. Li, H.; Feng, C.; Fan, C.; Yang, Y.; Yang, X.; Lu, H.; Lu, Q.; Zhu, F.; Xiang, C.; Zhang, Z.; et al. Intervention of oncostatin M-driven mucosal inflammation by berberine exerts therapeutic property in chronic ulcerative colitis. *Cell Death Dis.* **2020**, *11*, 271. [CrossRef] [PubMed]
22. West, N.R.; Hegazy, A.N.; Owens, B.M.J.; Bullers, S.J.; Linggi, B.; Buonocore, S.; Coccia, M.; Görtz, D.; This, S.; Stockenhuber, K.; et al. Oncostatin M drives intestinal inflammation and predicts response to tumor necrosis factor–neutralizing therapy in patients with inflammatory bowel disease. *Nat. Med.* **2017**, *23*, 579–589. [CrossRef] [PubMed]
23. Rittling, S.R.; Singh, R. Osteopontin in immune-mediated diseases. *J. Dent. Res.* **2015**, *94*, 1638–1645. [CrossRef]
24. Iida, T.; Wagatsuma, K.; Hirayama, D.; Nakase, H. Is osteopontin a friend or foe of cell apoptosis in inflammatory gastrointestinal and liver diseases? *Int. J. Mol. Sci.* **2018**, *19*, 7. [CrossRef] [PubMed]
25. Nakashima, A.; Yamada, K.; Iwata, O.; Sugimoto, R.; Atsuji, K.; Ogawa, T.; Ishibashi-Ohgo, N.; Suzuki, K. β-Glucan in foods and its physiological functions. *J. Nutr. Sci. Vitaminol.* **2018**, *64*, 8–17. [CrossRef] [PubMed]
26. Bai, J.; Ren, Y.; Li, Y.; Fan, M.; Qian, H.; Wang, L.; Wu, G.; Zhang, H.; Qi, X.; Xu, M.; et al. Physiological functionalities and mechanisms of β-glucans. *Trends Food Sci. Technol.* **2019**, *88*, 57–66. [CrossRef]
27. Suchecka, D.; Gromadzka-Ostrowska, J.; Żyła, E.; Harasym, J.; Oczkowski, M. Selected physiological activities and health promoting properties of cereal beta-glucans. A review. *J. Anim. Feed Sci.* **2017**, *26*, 183–191. [CrossRef]
28. Catana, C.S.; Magdas, C.; Tabaran, F.A.; Craciun, E.C.; Deak, G.; Magdas, V.A.; Cozma, V.; Gherman, C.M.; Berindan-Neagoe, I.; Dumitrascu, D.L. Comparison of two models of inflammatory bowel disease in rats. *Adv. Clin. Exp. Med.* **2018**, *27*, 599–607. [CrossRef]
29. Antoniou, E.; Margonis, G.A.; Angelou, A.; Pikouli, A.; Argiri, P.; Karavokyros, I.; Papalois, A.; Pikoulis, E. The TNBS-induced colitis animal model: An overview. *Ann. Med. Surg.* **2016**, *11*, 9–15. [CrossRef]
30. Ramos, G.P.; Papadakis, K.A. Mechanisms of Disease: Inflammatory Bowel Diseases. *Mayo Clin. Proc.* **2019**, *94*, 155–165. [CrossRef]
31. Chen, L.; Deng, H.; Cui, H.; Fang, J.; Zuo, Z.; Deng, J.; Li, Y.; Wang, X.; Zhao, L. Inflammatory responses and inflammation-associated diseases in organs. *Oncotarget* **2018**, *9*, 7204–7218. [CrossRef] [PubMed]
32. Żyła, E.; Dziendzikowska, K.; Kamola, D.; Wilczak, J.; Sapierzyński, R.; Harasym, J.; Gromadzka-Ostrowska, J. Anti-inflammatory activity of oat beta-glucans in a crohn's disease model: Time-and molar mass-dependent effects. *Int. J. Mol. Sci.* **2021**, *22*, 4485. [CrossRef] [PubMed]
33. Koelink, P.J.; Overbeek, S.A.; Braber, S.; De Kruijf, P.; Folkerts, G.; Smit, M.J.; Kraneveld, A.D. Targeting chemokine receptors in chronic inflammatory diseases: An extensive review. *Pharmacol. Ther.* **2012**, *133*, 1–18. [CrossRef] [PubMed]
34. Boshagh, M.A.; Foroutan, P.; Moloudi, M.R.; Fakhari, S.; Malakouti, P.; Nikkhoo, B.; Jalili, A. ELR positive CXCL chemokines are highly expressed in an animal model of ulcerative colitis. *J. Inflamm. Res.* **2019**, *12*, 167–174. [CrossRef]
35. Li, Q.; Lian, Y.; Deng, Y.; Chen, J.; Wu, T.; Lai, X.; Zheng, B.; Qiu, C.; Peng, Y.; Li, W.; et al. mRNA-engineered mesenchymal stromal cells expressing CXCR2 enhances cell migration and improves recovery in IBD. *Mol. Ther. Nucleic Acids* **2021**, *26*, 222–236. [CrossRef]
36. Majima, T.; Funahashi, Y.; Kawamorita, N.; Takai, S.; Matsukawa, Y.; Yamamoto, T.; Yoshimura, N.; Gotoh, M. Role of microglia in the spinal cord in colon-to-bladder neural crosstalk in a rat model of colitis. *Neurourol. Urodyn.* **2018**, *37*, 1320–1328. [CrossRef]
37. Sasaki, S.; Baba, T.; Shinagawa, K.; Matsushima, K.; Mukaida, N. Crucial involvement of the CCL3-CCR5 axis-mediated fibroblast accumulation in colitis-associated carcinogenesis in mice. *Int. J. Cancer* **2014**, *135*, 1297–1306. [CrossRef]
38. Miranda, P.M.; De Palma, G.; Serkis, V.; Lu, J.; Louis-Auguste, M.P.; McCarville, J.L.; Verdu, E.F.; Collins, S.M.; Bercik, P. High salt diet exacerbates colitis in mice by decreasing Lactobacillus levels and butyrate production. *Microbiome* **2018**, *6*, 57. [CrossRef]

39. Kopiasz, Ł.; Dziendzikowska, K.; Gajewska, M.; Wilczak, J.; Harasym, J.; Żyła, E.; Kamola, D.; Oczkowski, M.; Królikowski, T.; Gromadzka-Ostrowska, J. Time-dependent indirect antioxidative effects of oat beta-glucans on peripheral blood parameters in the animal model of colon inflammation. *Antioxidants* **2020**, *9*, 375. [CrossRef]
40. Xie, J.; Liu, Y.; Chen, B.; Zhang, G.; Ou, S.; Luo, J.; Peng, X. Ganoderma lucidum polysaccharide improves rat DSS-induced colitis by altering cecal microbiota and gene expression of colonic epithelial cells. *Food Nutr. Res.* **2019**, *63*, 1559. [CrossRef]
41. De Graaff, P.; Berrevoets, C.; Rösch, C.; Schols, H.A.; Verhoef, K.; Wichers, H.J.; Debets, R.; Govers, C. Curdlan, zymosan and a yeast-derived β-glucan reshape tumor-associated macrophages into producers of inflammatory chemo-attractants. *Cancer Immunol. Immunother.* **2021**, *70*, 547–561. [CrossRef] [PubMed]
42. Dent, G.; Loweth, S.C.; Hasan, A.M.; Leslie, F.M. Synergic production of neutrophil chemotactic activity by colonic epithelial cells and eosinophils. *Immunobiology* **2014**, *219*, 793–797. [CrossRef] [PubMed]
43. Prame Kumar, K.; Nicholls, A.J.; Wong, C.H.Y. Partners in crime: Neutrophils and monocytes/macrophages in inflammation and disease. *Cell Tissue Res.* **2018**, *371*, 551–565. [CrossRef] [PubMed]
44. Żyła, E.; Dziendzikowska, K.; Gajewska, M.; Wilczak, J.; Harasym, J.; Gromadzka-Ostrowska, J. Beneficial effects of oat beta-glucan dietary supplementation in colitis depend on its molecular weight. *Molecules* **2019**, *24*, 3591. [CrossRef] [PubMed]
45. Kühl, A.A.; Kakirman, H.; Janotta, M.; Dreher, S.; Cremer, P.; Pawlowski, N.N.; Loddenkemper, C.; Heimesaat, M.M.; Grollich, K.; Zeitz, M.; et al. Aggravation of Different Types of Experimental Colitis by Depletion or Adhesion Blockade of Neutrophils. *Gastroenterology* **2007**, *133*, 1882–1892. [CrossRef]
46. Zhang, R.; Ito, S.; Nishio, N.; Cheng, Z.; Suzuki, H.; Isobe, K. ichi Up-Regulation of Gr1+CD11b+ population in spleen of dextran sulfate sodium administered mice works to repair colitis. *Inflamm. Allergy Drug Targets* **2011**, *10*, 39–46. [CrossRef]
47. Kopiasz, Ł.; Dziendzikowska, K.; Gajewska, M.; Oczkowski, M.; Majchrzak-Kuligowska, K.; Królikowski, T.; Gromadzka-Ostrowska, J. Effects of dietary oat beta-glucans on colon apoptosis and autophagy through tlrs and dectin-1 signaling pathways—Crohn's disease model study. *Nutrients* **2021**, *13*, 321. [CrossRef]
48. Li, M.; Sun, X.; Zhao, J.; Xia, L.; Li, J.; Xu, M.; Wang, B.; Guo, H.; Yu, C.; Gao, Y.; et al. CCL5 deficiency promotes liver repair by improving inflammation resolution and liver regeneration through M2 macrophage polarization. *Cell. Mol. Immunol.* **2020**, *17*, 753–764. [CrossRef]
49. Wang, Q.; Zhang, T.; Chang, X.; Lim, D.Y.; Wang, K.; Bai, R.; Wang, T.; Ryu, J.; Chen, H.; Yao, K.; et al. ARC is a critical protector against inflammatory bowel disease (IBD) and IBD-associated colorectal tumorigenesis. *Cancer Res.* **2020**, *80*, 4158–4171. [CrossRef]
50. Sahu, B.D.; Kumar, J.M.; Sistla, R. Fisetin, a dietary flavonoid, ameliorates experimental colitis in mice: Relevance of NF-κB signaling. *J. Nutr. Biochem.* **2016**, *28*, 171–182. [CrossRef]
51. Yu, C.; Zhang, S.; Wang, Y.; Zhang, S.; Luo, L.; Thorlacius, H. Platelet-Derived CCL5 Regulates CXC Chemokine Formation and Neutrophil Recruitment in Acute Experimental Colitis. *J. Cell. Physiol.* **2016**, *231*, 370–376. [CrossRef] [PubMed]
52. Nieto, J.C.; Zamora, C.; Cantó, E.; Garcia-Planella, E.; Gordillo, J.; Ortiz, M.A.; Juárez, C.; Vidal, S. CSF-1 regulates the function of monocytes in Crohn's disease patients in remission. *Sci. Rep.* **2017**, *7*, 92. [CrossRef] [PubMed]
53. Mencarelli, A.; Cipriani, S.; Francisci, D.; Santucci, L.; Baldelli, F.; Distrutti, E.; Fiorucci, S. Highly specific blockade of CCR5 inhibits leukocyte trafficking and reduces mucosal inflammation in murine colitis. *Sci. Rep.* **2016**, *6*, 30802. [CrossRef] [PubMed]
54. Savić Mlakar, A.; Hojsak, I.; Jergović, M.; Čimić, S.; Bendelja, K. Pediatric Crohn disease is characterized by Th1 in the terminal ileum and Th1/Th17 immune response in the colon. *Eur. J. Pediatr.* **2018**, *177*, 611–616. [CrossRef] [PubMed]
55. Xiao, H.T.; Peng, J.; Wen, B.; Hu, D.D.; Hu, X.P.; Shen, X.C.; Liu, Z.G.; He, Z.D.; Bian, Z.X. Indigo Naturalis Suppresses Colonic Oxidative Stress and Th1/Th17 Responses of DSS-Induced Colitis in Mice. *Oxid. Med. Cell. Longev.* **2019**, *2019*, 9480945. [CrossRef]
56. Ye, X.; Liu, S.; Hu, M.; Song, Y.; Huang, H.; Zhong, Y. CCR5 expression in inflammatory bowel disease and its correlation with inflammatory cells and β-arrestin2 expression. *Scand. J. Gastroenterol.* **2017**, *52*, 551–557. [CrossRef]
57. Oz, H.S.; Zhong, J.; De Villiers, W.J.S. Osteopontin ablation attenuates progression of colitis in TNBS model. *Dig. Dis. Sci.* **2012**, *57*, 1554–1561. [CrossRef]
58. Toyonaga, T.; Nakase, H.; Ueno, S.; Matsuura, M.; Yoshino, T.; Honzawa, Y.; Itou, A.; Namba, K.; Minami, N.; Yamada, S.; et al. Osteopontin deficiency accelerates spontaneous colitis in mice with disrupted gut microbiota and macrophage phagocytic activity. *PLoS ONE* **2015**, *10*, e0135552. [CrossRef]
59. Wei, F.; Lang, Y.; Shen, Q.; Xu, L.; Cheng, N.; Chu, Y.; Lyu, H.; Chen, F. Osteopontin-loaded PLGA nanoparticles enhance the intestinal mucosal barrier and alleviate inflammation via the NF-κB signaling pathway. *Colloids Surf. B Biointerfaces* **2020**, *190*, 110952. [CrossRef]
60. Tang, R.; Yang, G.; Zhang, S.; Wu, C.; Chen, M. Opposite effects of interferon regulatory factor 1 and osteopontin on the apoptosis of epithelial cells induced by TNF-α in inflammatory bowel disease. *Inflamm. Bowel Dis.* **2014**, *20*, 1950–1961. [CrossRef]
61. Hamilton, J.A.; Cook, A.D.; Tak, P.P. Anti-colony-stimulating factor therapies for inflammatory and autoimmune diseases. *Nat. Rev. Drug Discov.* **2016**, *16*, 53–70. [CrossRef] [PubMed]
62. Meshkibaf, S.; Martins, A.J.; Henry, G.T.; Kim, S.O. Protective role of G-CSF in dextran sulfate sodium-induced acute colitis through generating gut-homing macrophages. *Cytokine* **2016**, *78*, 69–78. [CrossRef] [PubMed]
63. Harasym, J.; Żyła, E.; Dziendzikowska, K.; Gromadzka-Ostrowska, J. Proteinaceous Residue Removal from Oat β-Glucan. *Molecules* **2019**, *24*, 1729. [CrossRef] [PubMed]

Warszawa, 13.11.2023 r.

Łukasz Kopiasz
lukasz_kopiasz@sggw.edu.pl

Rada Dyscypliny Technologii Żywności i Żywienia

Szkoły Głównej Gospodarstwa Wiejskiego w Warszawie

Oświadczenie o współautorstwie

Niniejszym oświadczam, że w pracy Łukasz Kopiasz, Katarzyna Dziendzikowska, Michał Oczkowski, Joanna Harasym, Joanna Gromadzka-Ostrowska (2023). *Low molar-mass oat beta-glucan impacts autophagy and apoptosis in early stages of induced colorectal carcinogenesis in rats.* International Journal of Biological Macromolecules, 254:127832. doi: 10.1016/j.ijbiomac.2023.127832 mój indywidualny udział w jej powstaniu polegał na przeprowadzeniu doświadczenia *in vivo* (główny wykonawca), wykonaniu analiz immunohistochemicznych i Western blot, opracowaniu statystycznym i opisaniu wszystkich wyników, wizualizacji i napisaniu oryginalnego draftu artykułu, dyskusji wyników, prowadzeniu korespondencji z wydawcą.

Łukasz Kopiasz

Podpis

Warszawa, 13.11.2023

Katarzyna Dziendzikowska
katarzyna_dziendzikowska@sggw.edu.pl

Rada Dyscypliny Technologii Żywności i Żywienia

Szkoły Głównej Gospodarstwa Wiejskiego w Warszawie

Oświadczenie o współautorstwie

Niniejszym oświadczam, że w pracy Łukasz Kopiasz, Katarzyna Dziendzikowska, Michał Oczkowski, Joanna Harasym, Joanna Gromadzka-Ostrowska (2023). *Low molar-mass oat beta-glucan impacts autophagy and apoptosis in early stages of induced colorectal carcinogenesis in rats.* International Journal of Biological Macromolecules, 254:127832. doi: 10.1016/j.ijbiomac.2023.127832 mój indywidualny udział w jej powstaniu polegał na przeprowadzeniu doświadczenia in vivo, wykonaniu analizy ekspresji genów, wykonaniu analizy dyskryminacyjnej Fisher'a, edycji i korekcie merytorycznej artykułu.

Katarzyna Dziendzikowska

Podpis

Warszawa, 14.11.2023 r.

Michał Oczkowski
michal_oczkowski@sggw.edu.pl

Rada Dyscypliny Technologii Żywności i Żywienia

Szkoły Głównej Gospodarstwa Wiejskiego w Warszawie

Oświadczenie o współautorstwie

Niniejszym oświadczam, że w pracy Łukasz Kopiasz, Katarzyna Dziendzikowska, Michał Oczkowski, Joanna Harasym, Joanna Gromadzka-Ostrowska (2023). *Low molar-mass oat beta-glucan impacts autophagy and apoptosis in early stages of induced colorectal carcinogenesis in rats.* International Journal of Biological Macromolecules, 254:127832. doi: 10.1016/j.ijbiomac.2023.127832 mój indywidualny udział w jej powstaniu polegał na przeprowadzeniu doświadczenia *in vivo,* wykonaniu analizy Western blot.

Podpis

Michał Oczkowski

UNIWERSYTET EKONOMICZNY
WE WROCŁAWIU
Katedra Biotechnologii i Analizy Żywności
ul. Komandorska 118/120
53-345 Wrocław
(1)

Wrocław, 14.11.2023

Joanna Harasym
joanna.harasym@ue.wroc.pl

Rada Dyscypliny Technologii Żywności i Żywienia

Szkoły Głównej Gospodarstwa Wiejskiego w Warszawie

Oświadczenie o współautorstwie

Niniejszym oświadczam, że w pracy Łukasz Kopiasz, Katarzyna Dziendzikowska, Michał Oczkowski, Joanna Harasym, Joanna Gromadzka-Ostrowska (2023). *Low molar-mass oat beta-glucan impacts autophagy and apoptosis in early stages of induced colorectal carcinogenesis in rats.* International Journal of Biological Macromolecules, 254:127832. doi: 10.1016/j.ijbiomac.2023.127832 mój indywidualny udział w jej powstaniu polegał na wyizolowaniu beta-glukanów z owsa o małej masie molowej do doświadczenia *in vivo*, oznaczeniu zawartości beta-glukanów w paszy, edycji i korekcie merytorycznej artykułu.

KIEROWNIK KATEDRY
Biotechnologii i Analizy Żywności
dr hab. inż. Joanna Harasym, prof. UEW

Podpis

Warszawa, 14.11.2023 r.

Joanna Gromadzka-Ostrowska
joanna_gromadzka-ostrowska@sggw.edu.pl

Rada Dyscypliny Technologii Żywności i Żywienia

Szkoły Głównej Gospodarstwa Wiejskiego w Warszawie

Oświadczenie o współautorstwie

Niniejszym oświadczam, że w pracy Łukasz Kopiasz, Katarzyna Dziendzikowska, Michał Oczkowski, Joanna Harasym, Joanna Gromadzka-Ostrowska (2023). *Low molar-mass oat beta-glucan impacts autophagy and apoptosis in early stages of induced colorectal carcinogenesis in rats.* International Journal of Biological Macromolecules, 254:127832. doi: 10.1016/j.ijbiomac.2023.127832 mój indywidualny udział w jej powstaniu polegał na opracowaniu koncepcji badania, edycji i korekcie merytorycznej artykułu

Podpis

International Journal of Biological Macromolecules 254 (2024) 127832

Contents lists available at ScienceDirect

International Journal of Biological Macromolecules

journal homepage: www.elsevier.com/locate/ijbiomac

Low-molar-mass oat beta-glucan impacts autophagy and apoptosis in early stages of induced colorectal carcinogenesis in rats

Łukasz Kopiasz [a,*], Katarzyna Dziendzikowska [a], Michał Oczkowski [a], Joanna Harasym [b], Joanna Gromadzka-Ostrowska [a]

[a] Department of Dietetics, Institute of Human Nutrition Sciences, Warsaw University of Life Sciences, 02-776 Warsaw, Poland
[b] Department of Biotechnology and Food Analysis, Wroclaw University of Economics and Business, 53-345 Wroclaw, Poland

ARTICLE INFO

Keywords:
Oat beta-glucan
Colorectal cancer
Apoptosis

ABSTRACT

Oat beta-glucan is one of the soluble dietary fibre fractions with a wide spectrum of biological activities such as anti-inflammatory and anti-tumour properties. In the present study, the effect of low-molar-mass oat beta-glucan isolate (OβGl) on the level of autophagy and apoptosis in the colorectum of rats with induced early stages of colorectal cancer was investigated. Forty-five male Sprague-Dawley rats were divided into two main groups: control and azoxymethane-induced early-stage colorectal carcinogenesis (CRC). Both groups were divided into three dietary subgroups fed standard feed without OβGl (OβGl−), with 1 % of OβGl (OβGl+1 %) or with 3 % of OβGl (OβGl+3 %). The expression of autophagy (LC3B, beclin-1) and apoptosis (caspase-3, cleaved caspase-3, BAX, BCL-2 and PARP-1) markers was determined by immunohistochemistry, Western blot and PCR analysis. The obtained results showed that the expression of LC3B, caspase-3 and cleaved caspase-3 in the CRC mucosa, and LC3B-II expression in the CRC wall were higher in the OβGl+3 % compared to the OβGl− rats. A higher BAX/BCL-2 ratio was also observed in the CRC OβGl+1 % rats compared to the other CRC animals. In summary, OβGl+3 % has a modulatory effect, stimulating autophagy and the extrinsic apoptosis pathway, while OβGl+1 % has a stimulatory effect on the intrinsic apoptosis pathway.

1. Introduction

Colorectal cancer (CRC) is the third most common cancer worldwide and the second most common in terms of mortality [1]. According to data from the World Health Organization (WHO) in 2020, the number of new CRC cases exceeded 1.9 million, with the number of deaths surpassing 900,000 [2]. Both environmental and genetic factors determine the risk of developing CRC, but several studies particularly emphasize factors such as diet, lifestyle and family history as being particularly important in the development of CRC. Crucially, CRC can develop for many years without noticeable clinical symptoms, making both early medical diagnosis and the search for therapeutic and preventive agents that act at the early stages of carcinogenesis very important [3]. In fact, such agents could potentially include biologically active plant-derived compounds, such as oat beta-glucans [4].

Oat beta-glucans (OβG) are a dietary fibre fraction composed of D-glucose molecules linked by β-1,3, β-1,4 glycosidic bonds, resulting in a mostly linear structure with few branches. Due to their specific conformation, they exhibit many biological activities, such as anti-diabetic, prebiotic, cholesterol-lowering, anti-inflammatory, immunomodulatory and anti-tumour properties [4]. However, the anti-cancer effects of oat beta-glucans have only been confirmed in one in vivo study. In this study, Shen et al. [5] showed that OβG increased apoptosis in colon cells of mice with DMH-induced tumourigenesis. In addition, results from in vitro studies indicated strong anticancer activity of OβG against two human lung malignant tumour cell lines (A549, H69AR), malignant melanoma (Me45), epidermoid carcinoma (A431) and no toxicity to normal keratinocytes [6,7]. Moreover, they revealed pro-apoptotic properties against human melanoma HTB-140 cells [8]. Shah et al. [9] also showed increased anti-proliferative properties against human colon malignant tumour cells (Colo-205) with a decrease in the molar mass of barley beta-glucan, which has a similar structure and properties to oat beta-glucan. Besides, our previous studies (in animal models) have shown that OβG has anti-inflammatory [10–12],

* Corresponding author.
E-mail addresses: lukasz_kopiasz@sggw.edu.pl (Ł. Kopiasz), katarzyna_dziendzikowska@sggw.edu.pl (K. Dziendzikowska), michal_oczkowski@sggw.edu.pl (M. Oczkowski), joanna.harasym@ue.wroc.pl (J. Harasym), ostrowska@sggw.edu.pl (J. Gromadzka-Ostrowska).

https://doi.org/10.1016/j.ijbiomac.2023.127832
Received 16 May 2023; Received in revised form 25 October 2023; Accepted 30 October 2023
Available online 2 November 2023

antioxidative [13,14] and prebiotic [15] effects. These studies indicate that the low-molar-mass fraction has all of the above-mentioned properties, and in many cases, shows higher activity than the high-molar-mass fraction. Furthermore, in our previous study, we demonstrated the effect of OβG on apoptosis and autophagy in the colon altered by induced inflammation [16]. As it is known, chronic inflammation of the colon can lead to the development of cancer. Therefore, the evaluation of the impact of OβG in a colorectal cancer model was the natural continuation of our previous research.

Cancer is characterised by the accumulation of abnormal cells, resulting from an imbalance between cell proliferation, repair processes and programmed cell death. In cancer, a decrease in the apoptosis process is observed, which promotes the survival and replication of potential cancer cells. Therefore, the normal process of programmed cell death, which is regulated by a cascade of intracellular biochemicals, is essential to prevent tumour formation [17]. The key players in this process are caspases, the family of cysteine-aspartic proteases involved in the initiation or execution phases of apoptosis [18]. Caspase-3 (CASP-3) is one of the most important enzymes in the apoptotic process, linking both intrinsic and extrinsic pathways as a key executive enzyme. Activation of CASP-3 makes the apoptosis irreversible, therefore an active form of caspase-3 (cleaved caspase-3 (cCASP-3)) is the best marker to assess for intensity of this process in tissues [19]. A critical step in the activation of the intrinsic apoptotic pathway is the release of cytochrome C from the mitochondria into the cytoplasm, leading to the formation of the apoptosome and the activation of caspase-3. The release of cytochrome C is stimulated by pro-apoptotic members of the B-cell lymphoma protein 2 (BCL-2) family such as BCL-2-associated X (BAX), BCL-2-antagonist/killer 1 (BAK1) and inhibited by anti-apoptotic members of the same family such as BCL-2, B-cell lymphoma-extra-large (BCL-XL) [20]. Poly(ADP-ribose) polymerase-1 (PARP-1) is one of the DNA repair proteins which detects and repairs DNA damage, thus protecting cells against tumour induction. On the other hand, PARP-1 may have tumour-promoting effects through its ability to maintain and drive inflammation via the innate immune response and promote tumour growth [21].

Autophagy is a catabolic process of massive degradation and the removal of cellular components, including damaged/abnormal proteins and peptides. This process is also closely linked to many fundamental cellular processes such as the regulation of cell death, proliferation, inflammation as well as many innate and adaptive immune functions. Furthermore, it is regarded as a suppressive mechanism during tumour initiation and malignant transformation. Because of this wide spectrum of activity, dysregulation of autophagy has been associated with ageing and various diseases such as cancer, neurodegenerative disorders and chronic inflammatory diseases [22,23]. Microtubule-associated proteins 1A/1B-light chain 3 (LC3s) are structural components of autophagosomal membranes. In the cell, this protein exists in three forms: pro-LC3, LC3-I and LC3-II. When autophagy is initiated, the LC3-I form is converted to LC3-II, and the level of LC3-II is directly correlated with the number of autophagosomes formed. The LC3 protein exists in three forms in mammalian cells: LC3A, LC3B and LC3C. However, the best-studied endogenous autophagic marker in the literature is LC3B [24]. Another important autophagy-associated protein is beclin-1 (BECN-1). BECN-1 plays an important role in initiating the autophagy process. It interacts with the anti-apoptotic protein BCL-2 to form the BCL-2-beclin-1 complex, thus also influencing the apoptotic process. Overexpression of BECN-1 inhibits tumour cell growth and tumour cell formation in vivo, making it also a reliable marker for evaluating the efficacy of anticancer agents [25,26]. Environmental factors, including dietary factors, can modulate both apoptosis and autophagy.

Given the above prerequisites, we hypothesised that the consumption of low-molar-mass oat beta-glucan modulates the process of autophagy and apoptosis in the early stages of colon carcinogenesis. The aim of the present study was to investigate the effect of two different doses (1 % and 3 % (*w/w*)) of low-molar-mass chemically pure oat β-glucan isolate (OβGl) on the activity of autophagy and apoptosis in the colorectum of rats with induced early stages of colorectal cancer (CRC). Early stage of CRC was induced by peritoneal injection of azoxymethane (AOM), a highly specific carcinogen that induces colorectal tumours. Additionally, the AOM rat model of CRC possesses many characteristics found in human colon carcinogenesis [27].

2. Materials and methods

2.1. Preparation and characterization of low-molar-mass oat beta-glucan

A low-molar-mass oat 1–3, 1–4, beta-D-glucan preparation was obtained from oat bran (Bestpharma, Warszawa, Poland) by a patented method described in detail elsewhere [28,29]. Briefly, the raw material was frozen and then repeatedly milled in a frozen state to effectively reduce particle size. Subsequently, beta-glucan was isolated using alkaline water (pH = 8.5; NaOH). The remaining fraction was separated through centrifugation at 11,000 ×*g*. The supernatant was deproteinised at the isoelectric point (pH = 4.5), and the protein precipitate was removed by centrifugation. Further purification was performed by enzymatic treatment with a group of proteolytic, peptidolytic and amylolytic enzymes, followed by enzymatic precipitation of proteins at isoelectric points described in detail elsewhere [28]. The protein content (Lowry method) was negligible within the sensitivity range of the method (<0.01 mg/ml). The purity of the beta-glucan preparations was 99.3 %, characterised by an enzymatic methods (AACC Method 32-23.01, AOAC Method 995.16, AOAC Method 992.28, CODEX Method Type II, EBC Method 3.10.1, ICC Standard No. 166 and RACI Standard Method) and a molar mass of $5.2 \times 10^4 \pm 0.6 \times 10^4$ g/mol (52 ± 6 kDa) as characterised by size exclusion HPLC.

2.2. Animals and experimental design

The experiment was performed on adult (8 weeks old) male outbred (CRL:CD(SD)) Sprague-Dawley rats (n = 45) purchased from Charles River Laboratories (Sulzfeld, Germany). After one week of acclimatisation to the animal house conditions (temperature 22 ± 1 °C, relative humidity 50 ± 5 %, light/dark cycle 12/12 h, air exchange 15 times/h), the rats were separated into single-housed polycarbonate cages and divided into two main groups: an experimental group – rats with induced early stage of colorectal cancer (CRC, n = 24) and control group (C, n = 21). Early stage of colorectal cancer was induced by peritoneal injection of azoxymethane (AOM) (Sigma-Aldrich, Saint Louis, USA) once a week for two weeks [27]. In the control groups, an equal volume of 0.9 % saline solution was injected in the same manner. Animals from both experimental and control groups were divided into 3 dietary subgroups, according to the different content of low-molar-mass oat beta-glucans (OβGl) added to the standard AIN-93 M feed produced by ZooLab (Sędziszów, Poland) according to nutritional recommendation for rats [30]: (1) without OβGl (OβGl−), (2) with 1 % (*w/w*) of OβGl (OβGl+1 %) and (3) with 3 % (*w/w*) of OβGl (OβGl+3 %). Details of the oat beta-glucan content in the feed are shown in Supplementary Table 1 and the scheme of animal experiment is presented in Fig. 1. Feed was weighed at approximately 26 g per day (according to the available literature [31]) to prevent the rats from becoming obese throughout the experiment (8 weeks), and the measured average feed intake was 25.3 ± 0.6 g/day. Body weight gain was measured every 7 days, and the mean body weight gain was 28.8 ± 7.7 g/week. There were no significant differences in body weight and feed intake among the experimental groups (Supplementary Table 2 and Supplementary Fig. 1). Mean oat beta-glucan consumption is presented in Supplementary Table 3.

After 56 days of feeding the experimental or control feeds, the rats were bled from the heart under deep isoflurane (Aerrane Isoflurane USP, Baxter, Poland) anaesthesia. Subsequently, representative samples of the large intestine were collected by dividing them into three sections: the cecum, colon and rectum. A piece from each of these three sections

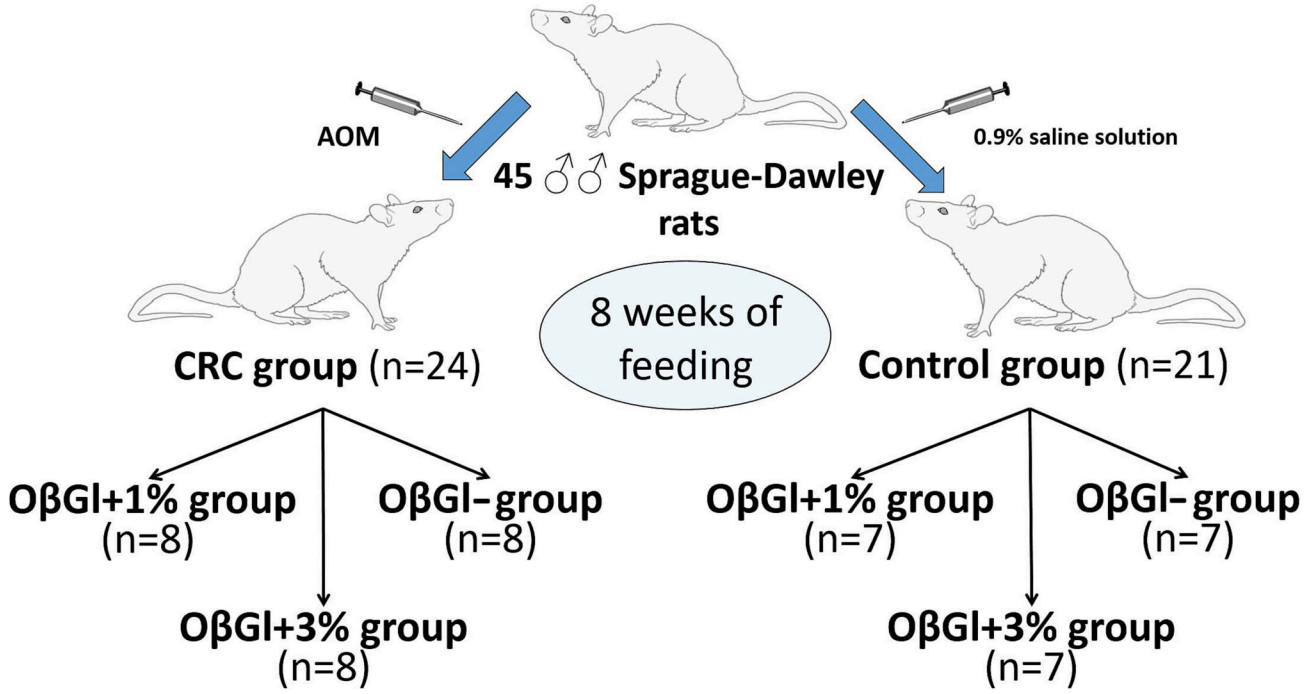

Fig. 1. Scheme of the study. AOM – azoxymethane, CRC – colorectal cancer (in this study AOM-induced early stage of colorectal carcinogenesis), OβGl+1 % – feed containing 1 % (*w/w/*) low-molar-mass oat beta-glucan, OβGl+3 % – feed containing 3 % (*w/w*) low-molar-mass oat beta-glucan, OβGl− – feed without low-molar-mass oat beta-glucan, ♂ – male gender, – peritoneal injection.

was taken and frozen together in liquid nitrogen for Western blot analysis, fixed together in 10 % buffered formaldehyde and embedded in paraffin for immunohistochemistry analysis, or dipped together in QIAzol lysis reagent (Qiagen, Hilden, Germany) and frozen in liquid nitrogen for Real-Time PCR analysis. All procedures were approved by the 2nd Local Ethics Committee in Warsaw (Resolution No. WAW2/040/2019) in accordance with the EU Directive 2010/63/EU for animal experiments and Polish law and 3Rs rules (*Replacement*, *Reduction and Refinement*).

2.3. Western blot analysis

Samples from three different parts of the large intestine from each rat were homogenised together in RIPA buffer (50 mM Tris, pH 7.5, 150 mM NaCl, 1 mM EDTA, 1 % NP-40, 0.25 % Na-deoxycholate, and 1 mM PMSF) supplemented with a cocktail of phosphatase and protease inhibitors (Sigma-Aldrich, Saint Louis, USA) using a tissue homogeniser (Bio-Gen PRO 200; PRO Scientific, Oxford, CT, USA). After the mechanical disruption of the tissue, the homogenates were incubated for 30 min at 4 °C on ice. The lysates were centrifuged at 14,000 rpm for 30 min and the supernatants were collected. The protein concentration in the lysates was determined using the Thermo Scientific™ Pierce™ BCA Protein Assay Kit according to the manufacturer's instructions (Thermo Scientific, Waltham, MA, USA). Next, the samples (normalised to 50 μg protein concentrations) were resolved by sodium dodecyl sulphate-polyacrylamide gel electrophoresis and transferred onto PVDF membrane (Bio-Rad, Hercules, CA, USA) using the TransBlot Turbo Transfer System (Bio-Rad, Hercules, CA, USA). The membranes were blocked for 10 min in EveryBlot Blocking Buffer (Bio-Rad, Waltham, MA, USA). Subsequently, they were incubated under gentle shaking at 4 °C overnight with primary antibodies (diluted in EveryBlot Blocking Buffer), including rabbit anti-LC3B polyclonal antibody (Cat#NB100-2220, 1:2000, Novus Biologicals, Littleton, CO, USA), rabbit anti-beclin-1 polyclonal antibody (Cat#A21695, 1:1250, ABclonal, Woburn, MA, USA), rabbit anti-caspase-3 polyclonal antibody (Cat#9662, 1:1000, Cell Signaling Technology, Danvers, MA, USA), rabbit anti-BCL-2 polyclonal antibody (Cat#PA5-27094, 1:1000, Invitrogen, Thermo Fisher Scientific, Inc., Waltham, MA, USA), mouse anti-BAX monoclonal antibody (Cat#MA5-14003, 1:200, Invitrogen, Thermo Fisher Scientific, Waltham, MA, USA), rabbit anti-PARP-1 polyclonal antibody (Cat#NBP2-13732, 1:1000, Novus Biologicals, Littleton, CO, USA) and mouse anti-β-actin (8H10D10) monoclonal antibody (Cat#3700, 1:5000, Cell Signaling Technology, Danvers, MA, USA). Following incubation, the membranes were washed three times for 5 min in Tris-Buffered Saline with 0.1 % Tween 20 Detergent and incubated with the appropriate secondary antibodies conjugated with IR fluorophores: IRDye® 680 (anti-mouse antibody) or IRDye® 800 CW (anti-rabbit antibody) (at 1:5000 dilution). The ChemiDoc Imaging System (Bio-Rad, Hercules, CA, USA) was used to analyse the protein expression. The instrument's scan resolution and intensity were set automatically. Quantification of the integrated optical density (IOD) was performed using the Image Lab 6.1 Software (Bio-Rad, Hercules, CA, USA). The relative levels of the analysed proteins were normalised to β-actin using a lane normalization factor calculated for each lane membrane according to the following formula from the iBright Imaging Systems technical note (Invitrogen, Thermo Fisher Scientific, Inc., Waltham, MA, USA):

Lane normalization factor = Observed signal of housekeeping protein for each lane/Highest observed signal of housekeeping protein on the blot

To normalise the signal of each experimental target band, the observed signal intensities of each experimental target band were divided by the lane normalization factor using the following formula:

$$\text{Normalized experimental signal} = \text{Observed experimental signal}/\text{Lane normalization factor}$$

object area were measured by using the NIS-Elements BR 5.01 program. The integrated optical density (IOD) was calculated using the following formula:

$$\text{Integrated Optical Density (IOD)} = \text{Object area}/\text{Measured area} \times \text{Mean saturation}$$

Finally, the normalised experimental signals were divided by 1,000,000 to obtain clearer results.

2.4. Immunohistochemical staining

Five-micrometre thick tissue slices containing three representative pieces of the large intestine from each rat were deparaffinised in xylene and rehydrated in a series of decreasing concentrations of ethanol. Subsequently, to recover antigens, the specimens were boiled twice for 5 min in citrate buffer (pH 6.0) in the microwave. Next, endogenous enzymes were blocked by incubation in the Bloxall Blocking Solution (Vector Laboratories, Burlingame, California, USA). After this procedure, the samples were incubated for 30 min at room temperature in 2,5 % Normal Horse Serum (Vector Laboratories, Burlingame, California, USA) followed by treatment with primary antibodies (diluted in 2,5 % Normal Horse Serum): rabbit anti-LC3B polyclonal antibody (Cat#NB100-2220, 1:1000, Novus Biologicals, Littleton, CO, USA), rabbit anti-beclin-1 polyclonal antibody (Cat#NB500-249, 1:1000, Novus Biologicals, Littleton, CO, USA), rabbit anti-caspase-3 polyclonal antibody (Cat#9662, 1:400, Cell Signaling Technology, Danvers, MA, USA), rabbit anti-cleaved caspase-3 polyclonal antibody (Cat#9661, 1:200, Cell Signaling Technology, Danvers, MA, USA), rabbit anti-BCL-2 polyclonal antibody (Cat#PA5-27094, 1:800, Invitrogen, Thermo Fisher Scientific, Waltham, MA, USA), mouse anti-BAX monoclonal antibody (Cat#MA5-14003, 1:300, Invitrogen, Thermo Fisher Scientific, Waltham, MA, USA), rabbit anti-PARP-1 polyclonal antibody (Cat#NBP2-13732, 1:500, Novus Biologicals, Littleton, CO, USA). The specimens were incubated with primary antibodies overnight at +4 °C. Subsequently, the samples were washed and labelled with polymers consisting of anti-rabbit or anti-mouse secondary antibodies conjugated to the horseradish peroxidase (HRP) enzyme complex (Vector Laboratories, Burlingame, California, USA). To obtain a brown colour, 3,3′-diaminobenzidine (DAB) was used. Hematoxylin was used for nuclei counterstaining.

2.5. Image analysis

The immunohistochemically stained slides were examined using a NIKON Eclipse Ti2 microscope (Nikon, Melville, NY, USA – funding details in Supplementary Data). The expression of the studied proteins was assessed in the colorectal mucosa because neoplastic lesions usually first affect the intestinal crypt cells and a rat model of AOM-induced CRC causes an increase in DNA mutations in colorectal epithelial cells [27]. On the recorded images, six mucosal areas for each of the three sections of the colorectum were marked. A total of eighteen marked mucosal areas for the colorectum from one rat were analysed together. Colorimetric saturation (brown colours reflecting antigen expression) and

The results present sample images of immunohistochemical preparations for each subgroup, corresponding to the average expression results obtained for the proteins studied. To better illustrate the observed changes in the expression of the proteins studied and the morphology of the colorectal mucosa, a magnification of ×400 was used.

2.6. RNA isolation, reverse transcription and real-time PCR

Total RNA was isolated from the colorectum samples using the RNeasy Lipid Tissue Mini Kit (Qiagen, Hilden, Germany) according to the manufacturer's instructions. The concentration and purity of RNA were assessed using a NanoDrop™ 2000 spectrophotometer (Thermo Fisher Scientific, Waltham, MA, USA). The integrity of several randomly selected samples of isolated RNA was measured on an Agilent Bioanalyzer 2100 system using a RNA 6000 Nano LabChip® kit (Agilent Technologies, Palo Alto, CA, USA). The analysis showed minimal RNA degradation, with a RNA integrity number (RIN) higher than 9. Subsequently, complementary DNA was synthesised using the RT2 First Strand Kit (Qiagen, Hilden, Germany). The pathway-focused gene expression analysis was performed using the Custom RT2 Profiler™ PCR array (Qiagen, Hilden, Germany) based on the manufacturer's instructions in two technical replicates for each colorectal sample. The RT2 Profiler PCR Arrays included primers for selected genes involved in apoptosis and autophagy processes (*Parp1*, cat. no PPR45370A; *Casp3*, cat. no PPR06384B; *Map1lc3b*, cat. no PPR49409A; *Becn-1*, cat. no PPR06523A; *Bax*, cat. no PPR06496C; *Bcl-2*, cat. no PPR06577B) (Qiagen, Hilden, Germany). Amplification was performed in the AriaMx Real-time PCR System (Agilent Technologies, Palo Alto, CA, USA) with an initial 10-min step at 95 °C followed by 40 cycles of 95 °C for 15 s and 60 °C for 1 min. Relative gene expression was calculated using the ΔΔCt method with B2m (cat. no PPR42607A) and Ldha (cat. no PPR56603B) as housekeeping genes in GeneGlobe Qiagen Software (Qiagen, Hilden, Germany). The results are presented as the relative gene expression of the target vs. reference gene (arithmetic mean), with the control group calculated as 1.

2.7. Statistical analysis

The obtained data were analysed using Statistica software (version 13.3 PL; StatSoft, Cracow, Poland). Normality of distribution and equality of variance were determined for all data. To enable statistical analysis, the following data were transformed to obtain the normal distribution and equal variance by the square root: Western blot results of cleaved PARP-1 and immunohistochemical results of caspase-3, cleaved caspase-3, BCL-2 and PARP-1. Two-way analysis of variance (ANOVA) was used to evaluate the influence of two experimental factors (early stage of colorectal cancer and type of dietary intervention) and the effect of an interaction between these factors. Furthermore, one-way

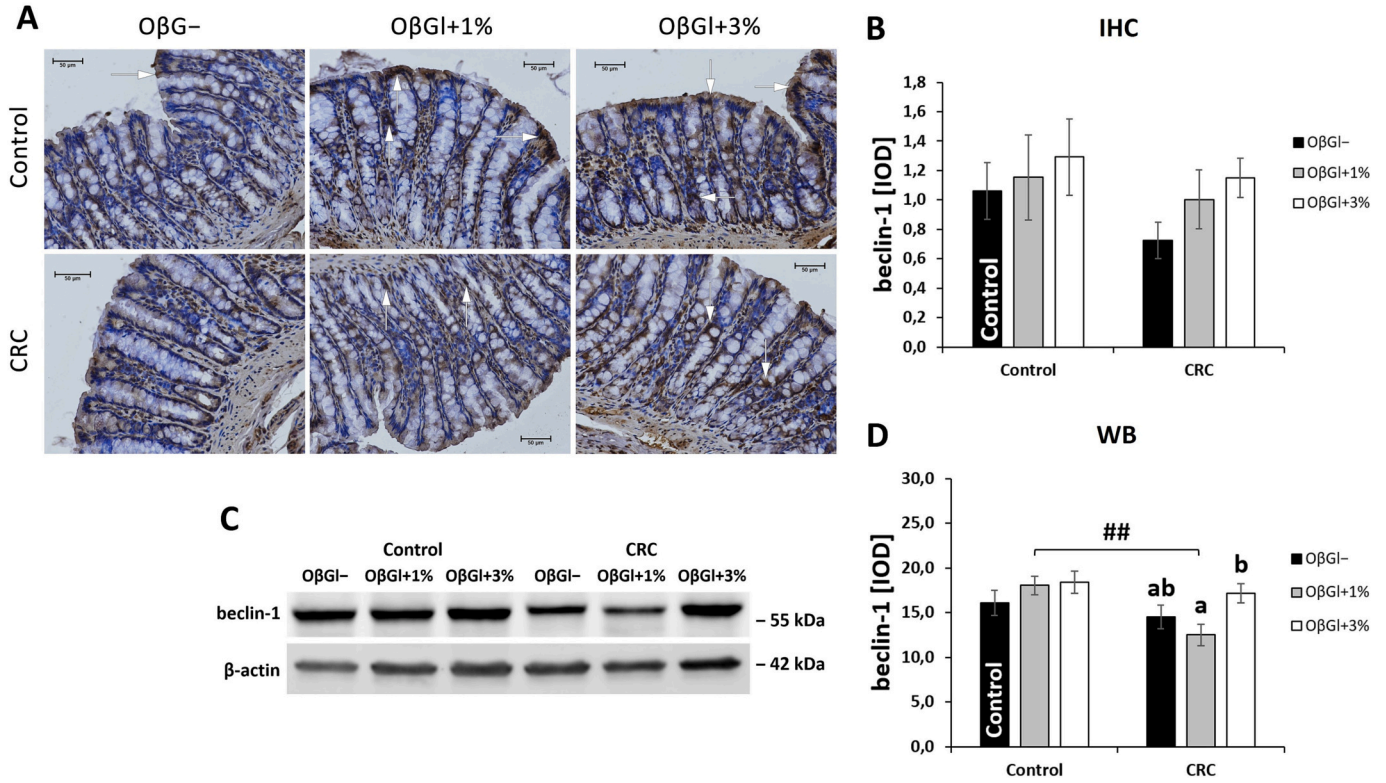

Fig. 2. Changes in beclin-1 protein expression in the colorectal mucosa (A-B) using immunohistochemistry analysis (IHC) and beclin-1 protein expression in the whole colorectal wall (C-D) using Western blot analysis (WB). (A) Light micrographs imaged (×400 magnification). White arrows indicate an area with a high expression of the beclin-1 (brown precipitate). (B) Changes in the expression of beclin-1 presented as integrated optical density (IOD), (mean ± SE). (C) Representative immunoblot images. (D) Changes in the expression of beclin-1 presented as IOD, (mean ± SE). Different letters denote significant differences among dietary subgroups in the control/CRC group determined by the Duncan post-hoc test ($^{a,b}p < 0.05$). Significant differences between the control and CRC groups on the same feed were determined by the Duncan post-hoc test ($^{\#\#}p < 0.01$). (For interpretation of the references to colour in this figure legend, the reader is referred to the web version of this article.)

ANOVA was used to test whether there were significant differences between the study subgroups. The significance of differences in results among the groups was determined by Tukey's post-hoc test. If Tukey's post hoc test showed no significant differences between subgroups, although the ANOVA *p*-value was <0.05, an additional Duncan's post hoc test was performed to complete the analysis of variance. The results of all dietary subgroups were compared with the control subgroup (OβG−) using Dunnett's post hoc test. Differences were considered significant when the p-value was <0.05.

Fisher's linear discriminant analysis (F-LDA) was conducted using R statistical software v. 3.3.3. (www.rproject.org/ (accessed on 13 August 2023)) (R: The R Project for Statistical Computing) that analysed the interaction between assessed parameters.

3. Results

3.1. Autophagy markers expression in the colorectum

The results of beclin-1 protein expression in the colorectal wall and colorectal mucosa are shown in Fig. 2. Analysis of variance showed no significant differences in immunohistochemically determined beclin-1 expression in the mucosa (Fig. 2B). However, significant differences in the expression of this protein were observed in the entire colorectal wall using the Western blot technique (Fig. 2C-D, ANOVA, $p < 0.05$). Duncan's post-hoc test showed that the expression of beclin-1 was lower in rats from the CRC group fed with feed containing 1 % low-molar-mass oat beta-glucan (OβGl+1 %) compared to the control group of rats fed the same feed. Consumption of feed containing 3 % oat beta-glucan in the CRC group resulted in significantly higher expression of beclin-1 compared to the CRC OβGl+1 % group and similar levels to the control group (Fig. 2D). In addition, low-molar-mass oat beta-glucan did not affect beclin-1 expression in the control groups.

The results of the expression of the major autophagosome formation marker (LC3B) are shown in Fig. 3. The expression of LC3B (LC3B-I and LC3B-II) in the mucosa was determined by immunohistochemical assay. Two-way ANOVA showed a significant interaction between the development of early stages of colorectal cancer and dietary intervention ($p < 0.01$). LC3B expression was higher in the mucosa of rats from the CRC group fed with feed containing 3 % OβGl compared to the control groups (control OβGl− and OβGl+3 %) and the CRC OβGl− group (Fig. 3B). The LC3B-II form, which directly correlates with the number of autophagosomes formed and is the most reliable autophagic marker, was determined in the entire colorectal wall using the Western blot. The results of the LC3B-II expression in the colorectal wall also showed a significantly higher expression of this protein in rats from the CRC OβGl+3 % group compared to the control groups (control OβGl− and OβGl+3 %) and the CRC OβGl− group. In addition, a higher expression of LC3B-II was observed in the CRC OβGl+3 % group than in the CRC OβGl+1 % group (Fig. 3D). OβGl had no influence on LC3B expression in the control groups. An analysis of LC3B-I expression was also performed. However, no significant statistical differences were found among the experimental groups (Supplementary Fig. 2).

3.2. Apoptosis markers expression in the colorectum

Immunohistochemical results show the expression of total (full-length and cleaved) caspase-3 (CASP-3) (Fig. 4A-B) and cleaved caspase-3 (cCASP-3) in the mucosa (Fig. 4C-D). Significant differences in

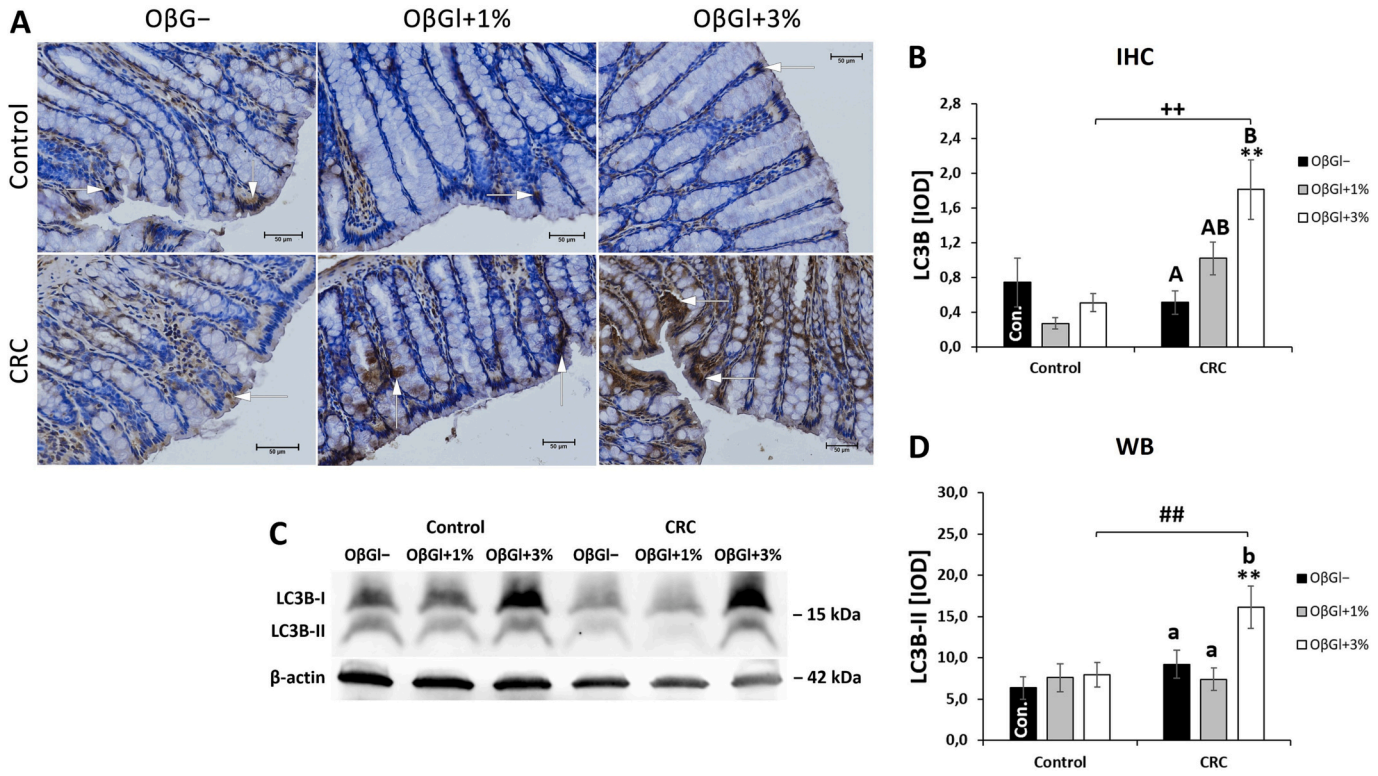

Fig. 3. Changes in LC3B expression in the colorectal mucosa (A-B) using immunohistochemistry analysis (IHC) and LC3B-II expression in the whole colorectal wall (C-D) using Western blot analysis (WB). (A) Light micrographs imaged (×400 magnification). White arrows indicate areas with high expression of the LC3B (brown precipitate). (B) Changes in the expression of LC3B presented as integrated optical density (IOD), (mean ± SE). (C) Representative immunoblot images. (D) Changes in the expression of LC3B-II presented as IOD, (mean ± SE). Different letters denote significant differences among dietary subgroups in the control/CRC group determined by Tukey post-hoc test ($^{A,B}p < 0.05$) or Duncan post-hoc test ($^{a,b}p < 0.05$). Significant differences between the control and CRC groups on the same feed were determined by the Tukey post hoc test ($^{++}p < 0.01$) or the Duncan post-hoc test ($^{\#\#}p < 0.01$). Significant differences from the control group (control OβGl−) were determined by the Dunnett post-hoc test ($^{**}p < 0.01$). (For interpretation of the references to colour in this figure legend, the reader is referred to the web version of this article.)

caspase-3 expression were observed for both cases, for CASP-3 and cCASP-3 (ANOVA, $p < 0.05$). Induction of early-stage colorectal carcinogenesis in rats resulted in lower CASP-3 expression in the mucosa compared to control rats but, this effect was only confirmed by Duncan's post-hoc test ($p < 0.05$), which has a high risk of type I error, and did not affect cCASP-3 expression. Significantly higher expression of CASP-3 was found in rats from CRC groups fed with feed supplemented with 1 % or 3 % OβGl compared to the CRC OβGl− group. However, the expression of cCASP-3 was only significantly higher in the CRC OβGl+3 % group compared to the control groups and other CRC groups. In all control groups, no changes in the expression of caspase-3 and cleaved caspase-3 in the colorectal mucosa were observed (Fig. 4B and D). Changes in cCASP-3 expression in the colorectal wall determined by Western blot analysis are shown in Fig. 4E-F. The expression of the active form of caspase-3 in the whole intestinal wall was higher only in the control OβGl+3 % group compared to the control OβGl+1 % and CRC OβGl+3 % groups. No differences were observed between the other subgroups.

The expression of BAX and BCL-2, markers of the intrinsic apoptotic pathway, is shown in Fig. 5. The results of ANOVA showed no significant differences in BAX expression in both the mucosa and the entire colorectal wall (Fig. 5B and F). In contrast, the changes in BCL-2 expression results were statistically significant in both the mucosa and the entire colorectal wall ($p < 0.05$). Furthermore, a two-way analysis of variance showed that the induction of early stages of colorectal cancer significantly influenced the decrease in BCL-2 expression in the colorectal wall ($p < 0.01$). Post-hoc analysis showed higher expression of BCL-2 protein in the mucosa of the CRC OβGl+3 % group compared to the CRC OβGl+1 % group (Fig. 5D). In addition, the expression of this protein was significantly lower in the entire colorectal wall in the rats from the CRC OβGl+1 % group compared to the control OβGl+1 % group (Fig. 5F). No changes in BAX and BCL-2 expression were observed in any of the control groups. Notably, the ratio of BAX to BCL-2 in the colorectal mucosa was significantly different among the study groups (ANOVA, $p < 0.05$). The BAX/BCL-2 expression ratio was higher in the CRC OβGl+1 % group than in the CRC OβGl− and OβGl+3 % groups (Fig. 5G).

3.3. Expression of PARP-1 in the colorectum

Fig. 6 shows changes in the expression of the DNA repair protein (poly(ADP-ribose) polymerase-1) in the colorectal mucosa determined by immunohistochemistry as well as full-length and cleaved forms of this protein in the whole colorectal wall determined by Western blot. According to the ANOVA results, the induction of early stages of colorectal cancer had a significant effect on the down-regulation of PARP-1 expression in the colorectal mucosa ($p < 0.01$) and the down-regulation of full-length PARP-1 expression in the whole colorectal wall ($p < 0.05$). Furthermore, significant changes in the expression of this protein between study subgroups were observed in the colorectal mucosa (ANOVA, $p < 0.05$). The expression of PARP-1 in the CRC OβGl− group was lower than in the control OβGl− group, whereas in the CRC OβGl+1 % and OβGl+3 % groups, the expression of this protein was similar to that observed in the control groups (Fig. 6B). No significant differences were observed among the study subgroups in the results of full-length and cleaved PARP-1 expression in the whole colorectal wall (Fig. 6D).

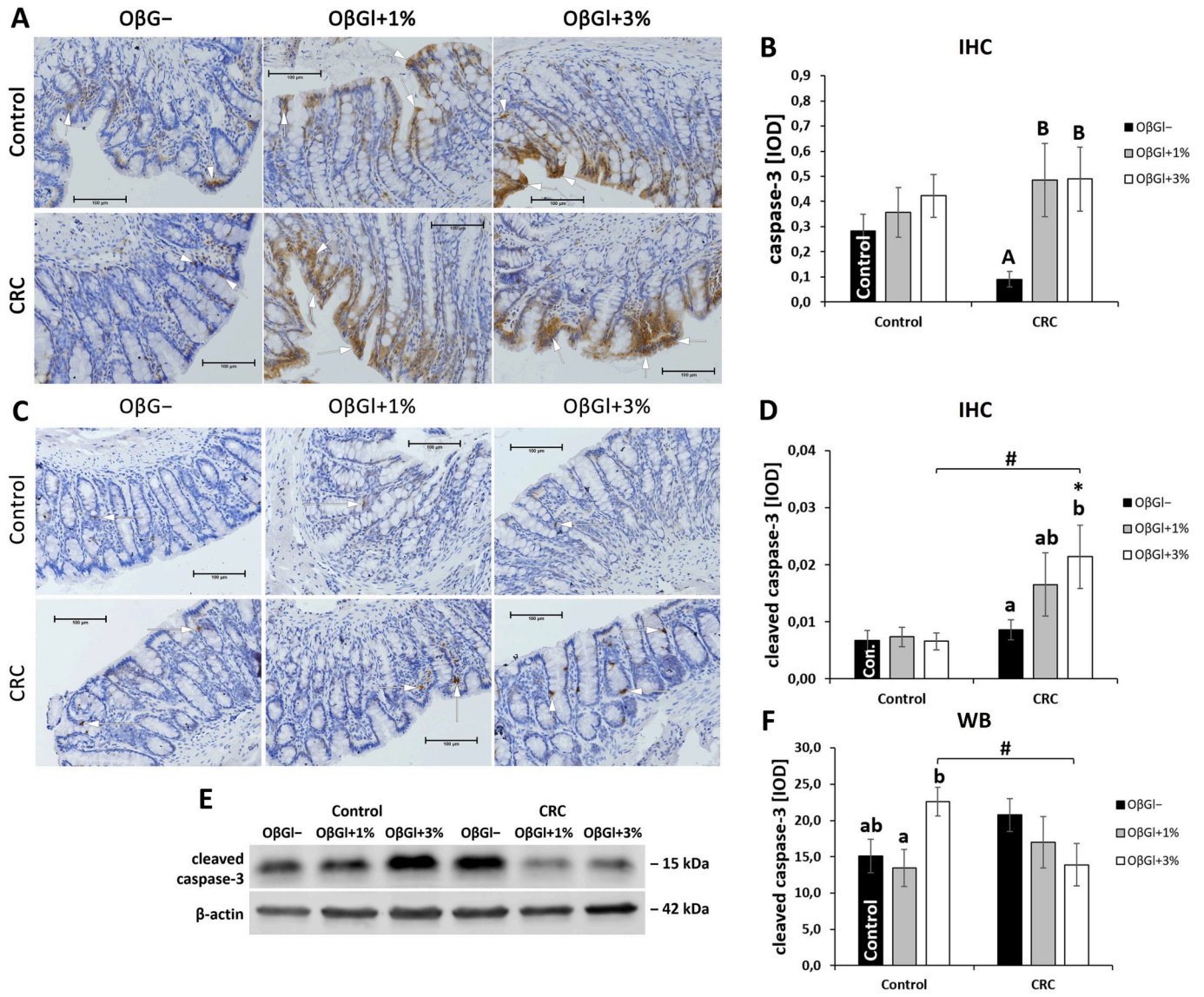

Fig. 4. Changes in total caspase-3 (A-B) and cleaved caspase-3 (C-D) expression in the colorectal mucosa using immunohistochemistry analysis (IHC) and cleaved caspase-3 expression in the whole colorectal wall (E-F) using Western blot analysis (WB). (A, C) Light micrographs imaged (×400 magnification). White arrows indicate areas with high expression of caspase-3 and cleaved caspase-3 (brown precipitate). (B, D) Changes in the expression of caspase-3 and cleaved caspase-3 presented as integrated optical density (IOD), (mean ± SE). (E) Representative immunoblot images. (F) Changes in the expression of cleaved caspase-3 presented as IOD, (mean ± SE). Different letters denote significant differences among dietary subgroups in the control/CRC group determined by Tukey post-hoc test ($^{A,B}p < 0.05$) or Duncan post-hoc test ($^{a,b}p < 0.05$). Significant differences between the control and CRC groups on the same feed were determined by the Duncan post-hoc test ($^{\#}p < 0.05$). Significant differences from the control group (control OβGl−) were determined by the Dunnett post-hoc test ($^{*}p < 0.05$). (For interpretation of the references to colour in this figure legend, the reader is referred to the web version of this article.)

3.4. Gene expression of autophagy, apoptosis and DNA repair markers in the colorectum

The results of the expression of genes associated with autophagy (*Lc3b* and *Becn-1*), apoptosis (*Casp-3*, *Bax*, *Bcl-2*) and DNA repair (*Parp-1*) markers in the colorectal tissue are shown in Fig. 7. Significant differences were found only for *Lc3b* gene expression (ANOVA $p < 0.05$, Fig. 7A) and insignificant differences for *Bcl-2* gene expression (ANOVA, tendency at $p = 0.066$, Fig. 7D). Two-way ANOVA showed that the induction of early stage of colorectal cancer had a significant influence on the decrease of *Lc3b* gene expression ($p < 0.01$). Post-hoc analysis showed that *Lc3b* gene expression was higher in rats from the CRC group fed with the control feed and the feed containing 1 % OβGl compared to the control groups (control OβG- and OβGl+1 %), while in the CRC OβGl+3 % group was at a similar level to the control groups.

3.5. Fisher's Linear Discriminant (FLD) analysis

FLD analysis was used to identify linear combinations of gene and protein expression of the analysed markers of autophagy and apoptosis, which allow the best separation between study groups. The method achieves the greatest possible separation between data groups by using the optimal linear combination of parameters used in the analysis. The results of the FLD analysis are shown in Fig. 8. Fig. 8A shows the results for six isolated experimental groups. The data are presented in the space between the linear combination of parameters (LDs) labelled LD_1 and LD_2, which best separate the previously defined groups.

The vectors in Fig. 8B indicate the direction and strength of the separation of the experimental groups as determined by the relevant parameters. The graphs show the parameters that had the greatest effect on separation. High values of the parameter corresponding to a given

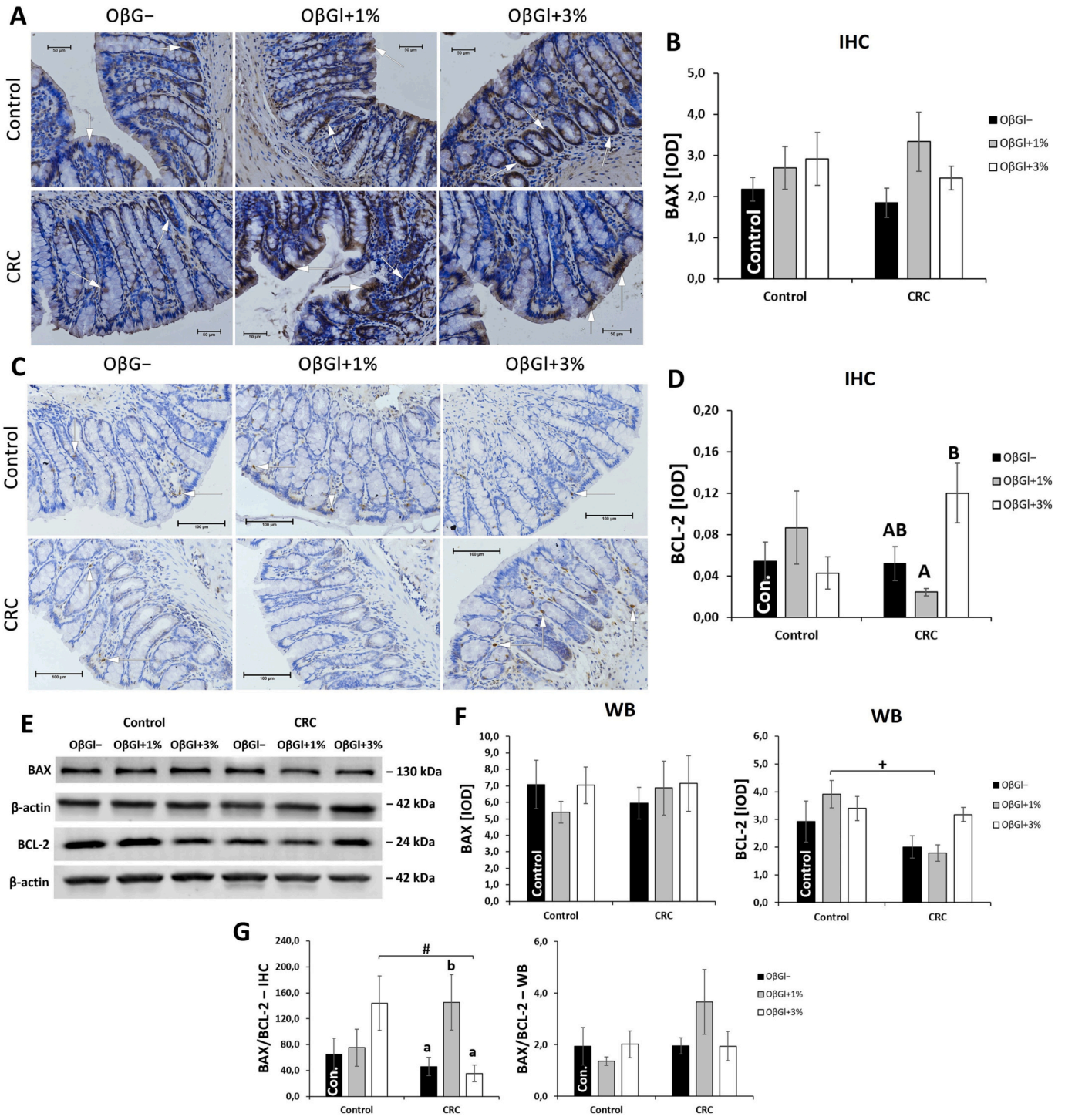

Fig. 5. Changes in BAX (A-B) and BCL-2 (C-D) expression in the colorectal mucosa using immunohistochemistry analysis (IHC) and BAX and BCL-2 expression in the whole colorectal wall (E-F) using western blot analysis (WB). (A, C) Light micrographs imaged (×400 magnification). White arrows indicate areas with high expression of the BAX and BCL-2 (brown precipitate). (B, D, F) Changes in the expression of BAX and BCL-2 presented as integrated optical density (IOD), (mean ± SE). (E) Representative immunoblot images. (G) Changes in the ratio of BAX to BCL-2 expression in colorectal mucosa (IHC) and colorectal wall (WB). Different letters denote significant differences among dietary subgroups in the control/CRC group determined by the Tukey post-hoc test ($^{A,B}p < 0.05$) or the Duncan post-hoc test ($^{a,b}p < 0.05$). Significant differences between the control and CRC groups with the same feed were determined by the Tukey post hoc test ($^{+}p < 0.05$) or the Duncan post-hoc test ($^{\#}p < 0.05$). (For interpretation of the references to colour in this figure legend, the reader is referred to the web version of this article.)

vector resulted in a shift of the data in the direction determined by the vector, and the length of the vector indicates the strength that the parameter exerted on the separation of the groups. The FLD analysis complemented the ANOVA and allowed the results to be summarised.

FLD analysis showed that the factors most differentiating the experimental groups were the protein expression of CASP-3, cCASP-3 and LC3B in the colorectal mucosa, BCL-2 and BECN-1 in the whole colorectal wall, and the gene expression of *Lc3b*, *Bcl-2* and *Bax/Bcl-2* in the colorectal tissue. The analysis showed that it was possible to identify a combination of the above parameters that allowed the control OβGl−

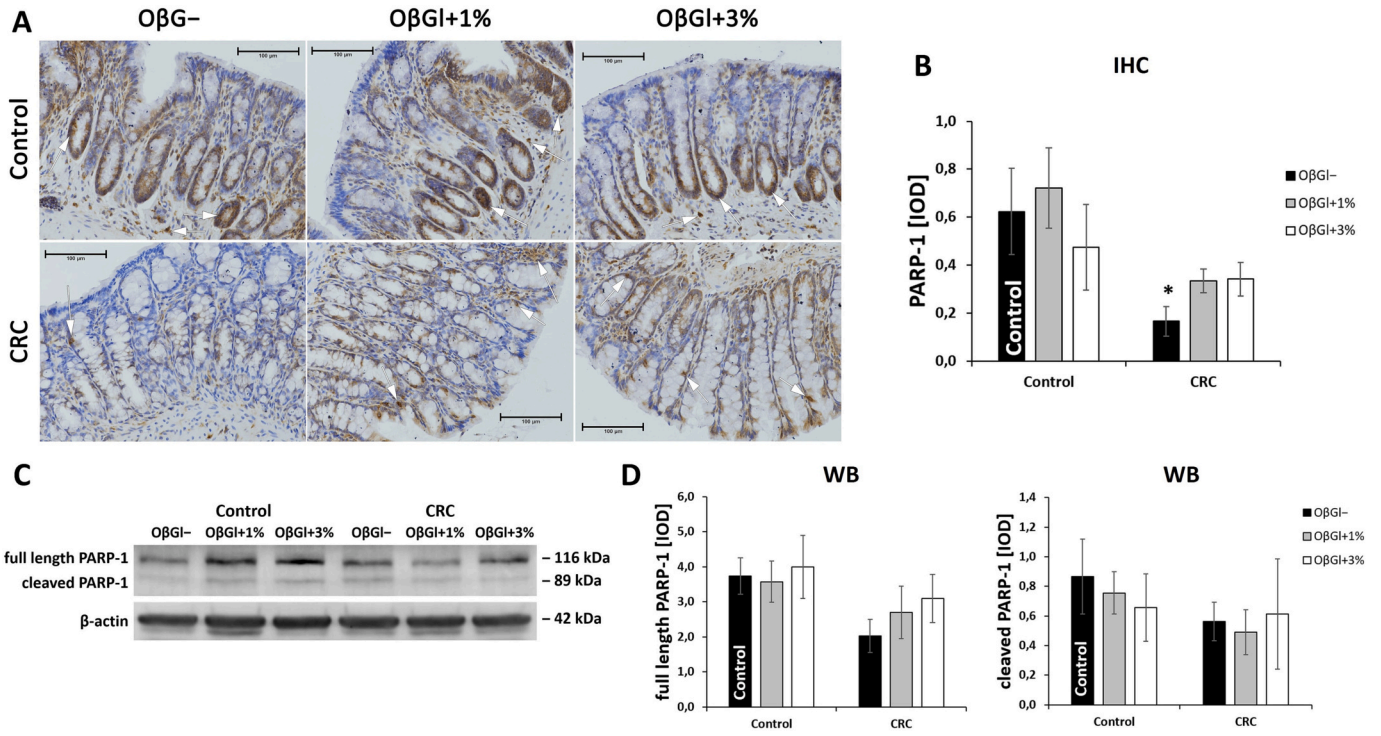

Fig. 6. Changes in PARP-1 expression in the colorectal mucosa (A-B) using immunohistochemistry analysis (IHC) and full length and cleaved PARP-1 expression in the whole colorectal wall (C-D) using Western blot analysis (WB). (A) Light micrographs imaged (×400 magnification). White arrows indicate areas with high expression of PARP-1 (brown precipitate). (B) Changes in the expression of PARP-1 presented as integrated optical density (IOD), (mean ± SE). (C) Representative immunoblot images. (D) Changes in the expression of full length and cleaved PARP-1 presented as IOD, (mean ± SE). Significant differences from the control group (control OβGl−) were determined by the Dunnett post-hoc test (*$p < 0.05$). (For interpretation of the references to colour in this figure legend, the reader is referred to the web version of this article.)

and OβGl+1 % groups to be separated from the CRC OβGl− and CRC OβGl+3 % groups, and to separate the CRC OβGl+1 % group from the other groups in the vertical plane (LD_2). The horizontal plane (LD_1) allowed a clear differentiation of the CRC OβGl+3 % group, as well as the separation of the CRC OβGl− group from the control groups and the CRC OβGl+1 % group. LC3B and CASP-3 expression in the colorectal mucosa and *Bcl-2* expression in the whole colorectal wall correlated most strongly with LD_1, *Lc3b* expression in the whole colorectal wall was correlated with LD_2, while the other parameters were correlated with both LDs. Thus, it can be concluded that the CRC OβGl+3 % group had significantly higher expression of LC3B and CASP-3 in the mucosa, and *Bcl-2* in the whole colorectal wall compared to the other study groups, with the largest difference from the CRC OβGl− group. In addition, this group also had a higher expression of cCASP-3 in the mucosa compared to the other groups. The direction of BCL-2 and BECN-1 expression vectors in the whole colorectal wall indicates lower values of the expression of these proteins in the CRC OβGl− and OβGl+1 % groups compared to the other groups. Moreover, FLD analysis shows a higher *Bax/Bcl-2* expression ratio in the CRC OβGl− and OβGl+1 % groups compared to the other groups, especially compared to the CRC OβGl+3 % group, while ANOVA showed no statistically significant differences.

4. Discussion

To the best of our knowledge, the present study is the first to describe the effects of high-purity low-molar-mass oat beta-glucan (OβGl) consumption on the early stages of colorectal cancer development. We investigated the effect of feed supplementation with this polysaccharide on markers of autophagy, apoptosis and DNA repair in the colorectum altered by the induction of carcinogenesis. In our study, AOM was used to induce CRC, particularly aberrant crypt foci, which are an early marker of CRC that begin to be present after 8–12 weeks following AOM exposure [27]. We used an 8-week protocol, thus obtaining a very early stage of carcinogenesis, in which aberrant crypts are just beginning to become visible histologically, which was observed in rats in the CRC group, confirming the efficacy of the animal model we constructed (Supplementary Fig. 3). The strength of our study lies in the use of two complementary analytical techniques to evaluate protein expression – Western blot and immunohistochemistry. Immunohistochemistry allowed us to assess the expression and localisation of the studied proteins in the colorectal mucosa, while Western blot provided an evaluation of protein expression throughout the entire colorectal wall. In the case of PARP-1, we were able to study the expression of both the full-length and cleaved forms, and in the case of LC3B, we assessed the expression of two isoforms, LC3B-I and LC3B-II. In our study, the early stage of carcinogenesis had little effect on the studied markers. However, it resulted in a significant reduction in the protein expression of CASP-3 and PARP-1 in the colorectal mucosa as well as full-length PARP-1 and BCL-2 in the entire colorectal wall. Not only that, CRC development decreased the relative gene expression of *Lc3b*. In the control groups, the consumption of OβGl+3 % caused only a slight increase in the expression of cleaved caspase-3 in the whole colorectal wall. The expression of the remaining proteins and their genes studied did not change in the control groups, indicating that OβGl has no effect on the normal colorectum. On the other hand, when combined with azoxymethane, oat beta-glucans caused significant changes in the expression of a larger number of studied proteins. Our results suggest that the OβGl stimulates the autophagy process during CRC development. This is indicated by the increased expression of LC3B in the colorectal mucosa and LC3B-II in the whole colorectal wall in rats with CRC development fed with feed containing 3 % OβGl. In addition, gene expression analysis showed that 3 % OβGl supplementation counteracted the reduction in *Lc3b* expression. Both 1 % and 3 % OβGl added to the feed increased the expression of caspase-3 in rat mucosa altered by

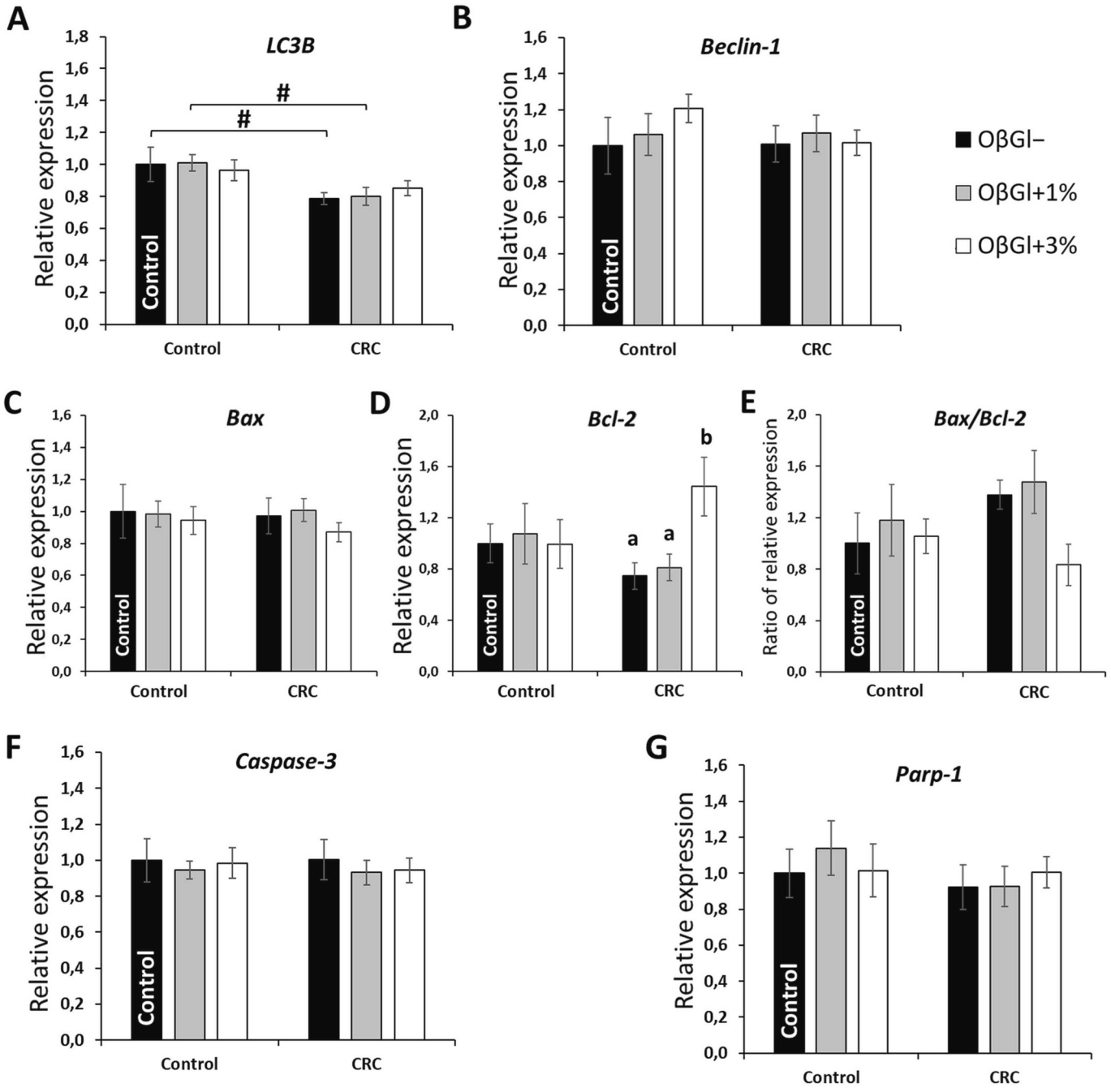

Fig. 7. Changes in relative gene expression of markers of autophagy (A-B), apoptosis (C-F), and DNA repair processes (G) in the colorectal tissue. Data are presented in arbitrary units as a ratio of the expression of the target gene to the mean expression of the reference genes (*B2m and Ldha*) with the control group calculated as 1. All values are presented as mean ± SE. Different letters denote significant differences among dietary subgroups in the control/CRC group determined by the Duncan post-hoc test ($^{a,b}p < 0.05$). Significant differences between the control and CRC groups with the same feed were determined by the Duncan post-hoc test ($^{\#}p < 0.05$).

CRC development, whereas only 3 % OβGl increased the expression of the active form of caspase-3. Analysis of the expression of cCASP-3 in the entire colon wall did not show such an effect, suggesting that the apoptosis stimulation by OβGl was limited to the colorectal mucosa. OβGl also counteracted the decreased expression of PARP-1, one of the essential DNA damage repair proteins, in the colorectal mucosa caused by the onset of carcinogenesis. Fisher's linear discriminant analysis, as a complement to ANOVA, confirmed the effect of OβGl on increased autophagy and apoptosis in the colon mucosa altered by cancer development. The higher expression of LC3B, CASP-3 and cCASP-3 in the colorectal mucosa was one of the main parameters that separated the CRC OβGl+3 % group from the CRC OβGl− group and other experimental groups. Moreover, several of the studied parameters were dose-dependent, particularly the protein expression of cleaved caspase-3, LC3B and BCL-2 in the mucosa, the protein expression of LC3B-II in the colorectal wall, as well as the gene expression of *Bcl-2*.

Autophagy may mediate cancer survival and progression by providing nutrients to cancer cells under the stress conditions. On the other hand, activation of autophagy may lead to cell death and inhibition of cancer progression. Depending on the stage of carcinogenesis, autophagy may act as a suppressor in the early stages or as a promoter in the advanced stages of cancer development [32,33]. In general, autophagy contributes to the suppression of tumour growth by removing damaged cells and cellular organelles, thereby limiting cell

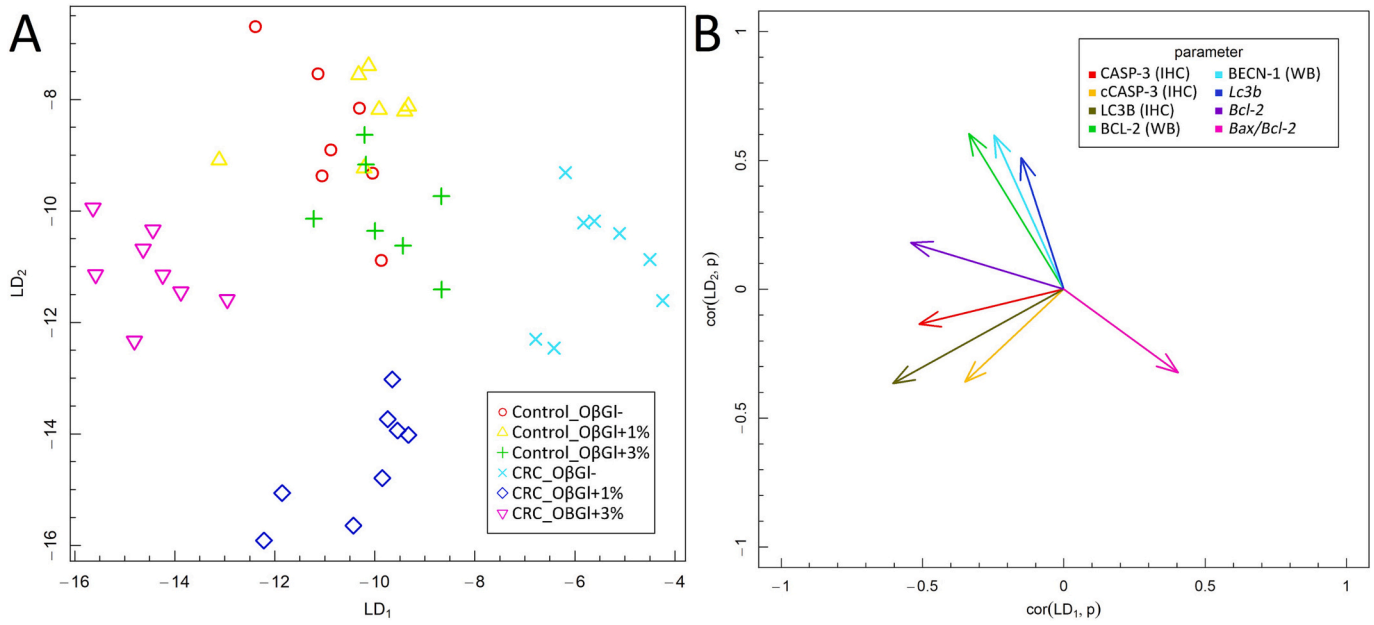

Fig. 8. Fisher's Linear Discriminant (FLD) analysis: (A) experimental data on the plane spanned by two of the most data-separating FLDs and (B) parameters contributing the most to FLDs. (IHC) indicate protein expression in colorectal mucosa marked by using immunohistochemical analysis; (WB) indicate protein expression in the whole colorectal wall marked by using Western blot analysis; italicized letters indicate gene expression.

proliferation, and genomic instability, which promotes tumour initiation [23]. Genomic instability is also one of the mechanisms of action of azoxymethane in CRC induction [27]. In our study, the enhancement of autophagy by the OβGl appeared to have a beneficial effect by reducing the risk of genomic instability and carcinogenesis initiation following exposure to AOM. An apparent effect of enhancing autophagy through an increase in LC3B and *Lc3b* expression was only observed in rats fed with feed containing 3 % OβGl. Additionally, the results of the FLD analysis indicate that the factors which differentiated the CRC OβGl+3 % group the most from the other groups were the increased expression of LC3B in the mucosa and LC3B-II expression in the whole colorectal wall. Whereas the addition of 1 % OβGl slightly affected the decreased expression of beclin-1 in the whole colorectal wall and the increased BAX/BCL-2 ratio in the colorectal mucosa altered by carcinogenesis. The effect of a lower dose of OβGl on beclin-1 expression may be related to the fact that the beclin-1 can be cleaved upon the increased expression of pro-apoptotic proteins such as caspases (-3, -7 and -8), or BAX, which is associated with the intrinsic apoptosis pathway [26].

The autophagy-stimulating effect of oat beta-glucan was demonstrated in in vivo studies using animal models of *colitis*. In our previous study, we induced colon inflammation in rats by rectal administration of 2,4,6-trinitrobensenosulfonic acid solution, creating an animal model of *colitis* similar to the human Crohn's disease. The results indicated that high-molar-mass oat beta-glucan exhibited autophagy-stimulating effects. Induced inflammation reduced LC3B expression after 21 days of the experiment, whereas in rats fed with feed containing high-molar-mass OβG, the expression of this protein was similar to that observed in the control group [16]. This effect is also confirmed by the recently published results of a study by other authors. Xu et al. [34] demonstrated the autophagy-promoting effect of OβG in a mouse model of inflammation induced by dextran sulphate sodium and in an in vitro model using human colorectal adenocarcinoma cells (HT-29) treated with LPS. The results showed a decreased expression of LC3B-II in intestinal epithelial cells and HT-29 cells under induced inflammation, while OβG increased LC3B-II expression to levels similar to the control group. In the above studies, the autophagy-stimulating effect was accompanied by the anti-inflammatory effects of OβG, resulting in reduced expression of pro-inflammatory cytokines such as TNF-α, IL-1β and IL-6 [10,16,34].

While autophagy's role in carcinogenesis remains controversial, with suggestions of both cancer-suppressive and cancer-promotion functions, apoptosis plays an anti-tumour role by inducing the death of cancer or potentially malignant cells [35]. The results of our study indicate that the process of apoptosis is enhanced in the colorectal mucosa altered by the early stage of carcinogenesis in the presence of OβGl. Both doses of OβGl (1 % and 3 %) caused a significant increase in caspase-3 expression in the colorectal mucosa with cancer development, while only the higher dose caused a significant increase in the active form of caspase-3. The FLD analysis confirmed this, as the high expression of cleaved caspase-3 in the mucosa was one of the factors that differentiated the experimental rats with induced CRC fed with feed containing 3 % OβGl from other rats. Furthermore, this effect was not observed in the whole colorectal wall, but only in the mucosa. Worth noting is the localisation of the cCASP-3 expression in the mucosa, primarily enhanced in the intestinal crypt cells in the presence of 3 % OβGl. These cells are the primary site of tumour initiation and transformation, leading to the formation of aberrant crypt foci [36]. Additional confirmation of the efficacy of OβG in stimulating apoptosis is provided by the results of the in vivo study published to date by Shen et al. [5]. These authors conducted a study on the effects of the soluble and insoluble fractions of oat beta-glucan at different doses in preventing colorectal cancer induced by 1,2-dimethylhydrazine in mice. The experimental period was 18 weeks, which resulted in visible colon tumour lesions on histological evaluation. The authors also analysed the effect of these polysaccharides on the apoptosis process of colon tumour cells using Annexin V and PI double staining. The results showed a significant effect of higher doses (100 mg/kg body weight) of both fractions of oat beta-glucan on increasing apoptosis. Several in vitro studies on various human cancer cell lines indicated anti-cancer properties, including pro-apoptotic effects of OβG. Choromańska et al. [6] showed that OβGl (6.965×10^4 g/mol), which has a similar molar mass to the beta-glucan used in our study, reduced the viability of human malignant melanoma (Me45) and epidermoid carcinoma (A431) cell lines with no effect on normal human keratinocytes (HaCaT). The reduction in viability of these cells was associated with increased expression of caspase-12 among other factors. Parzonko et al. [8] investigated the pro-apoptotic properties of OβGl (13.38×10^5

g/mol) against human skin cancer cells (HTB-140). The authors demonstrated a concentration-dependent effect of OβGl on the induction of apoptosis in HTB-140 cells, together with a significant activation of the effector caspase-3 and -7. Taken together, the enhancement of OβG-mediated programmed cell death at the early stages of colon carcinogenesis appears highly beneficial due to the increased removal of potentially cancerous cells. Notably, this effect was observed only in the mucosa, which is the most susceptible to neoplastic changes. Furthermore, as seen in the microscopic images, the increased expression of the active form of caspase-3 was limited to single cells within the intestinal crypts and was not extensive. This indicates a moderate level of apoptosis, which for example, should not affect the integrity of the intestinal barrier.

As it is well known, caspase-3 links both the intrinsic and extrinsic pathways of apoptosis. Cleaved caspase-3 is the most important of the apoptotic pathways as it acts as an executioner enzyme, making the process of programmed cell death irreversible [37]. Therefore, cleaved caspase-3 expression alone indicates the severity of the active apoptotic process, but does not determine which pathway it was induced. Both pathways play a crucial role in cancer prevention, but the intrinsic source of the signal initiating apoptosis, e.g. DNA damage, appears to be more important. Furthermore, some approved therapeutic agents, such as BCL-2 inhibitors, directly target the intrinsic apoptosis pathway [20]. The results of our study indicate a modulating effect of OβGl on BCL-2 expression and the ratio of BAX to BCL-2 expression. The rats with induced CRC fed with feed containing 3 % OβGl showed increased BCL-2 expression in the colorectal mucosa, with no effect on BAX expression and maintenance of a low BAX/BCL-2 ratio. This probably indicates that a high dose of OβGl has a non-stimulatory effect on the intrinsic apoptotic pathway and, in association with the increased expression of cleaved caspase-3, may enhance apoptosis by influencing the extrinsic pathway. In contrast, a lower dose of OβGl showed an effect on increasing the ratio of pro-apoptotic BAX to anti-apoptotic BCL-2, suggesting an increased release of cytochrome C from mitochondria and a stimulatory effect on the intrinsic apoptotic pathway. However, the results of cCASP-3 expression do not indicate an increase in active apoptosis of colorectal mucosa cells, which may be due to the very early stage of colorectal cancer development. Stimulation of the extrinsic apoptosis pathway may also be related to the immunomodulatory effect of OβG. As shown by the results of Zhang et al. [38], OβG with a mass of 200 kDa indicates a strong anti-tumour effect against melanoma with lung metastasis in mice. This effect was associated with a strong immunomodulatory effect in the tumour environment, including increased levels of inflammatory factors such as interferon-gamma (IFN-γ), tumour necrosis factor-alpha (TNF-α) and interferon regulatory factor 1 (IRF-1), as well as increased tumour infiltration by granzyme B produced by T cells. These factors are involved in the induction of apoptosis by the extrinsic pathway, particularly TNF-α, which binds to one of the death receptors – tumour necrosis factor receptors (TNFR1 and TNFR2) on the cell membrane surface [20,39]. The linkage of TNF-α with TNFR1/2 initiates a caspase-related apoptosis cascade that ultimately leads to caspase-3 activation and cell death [37]. In addition, granzyme B can induce tumour cell apoptosis through various pathways, including direct and indirect activation of the caspase-associated apoptosis cascade, and can also directly cleave procaspase-3 to the active form [40]. Furthermore, our previous study in an animal model of *colitis* demonstrated an inhibitory effect on excessive apoptosis after 7 days of the experiment, a period when the expression of cleaved caspase-3 was highest in inflamed intestinal epithelial cells [16]. It is worth noting that the effect was stronger for low-molar-mass oat beta-glucan, which also showed a more pronounced anti-inflammatory effect, leading to a greater reduction in the expression of pro-inflammatory factors, including TNF-alpha [10,12].

One of the potential mechanisms underlying the pro-apoptotic effect of OβGl may be its influence on the gut microbiota, resulting in increased production of SCFAs. Both in vitro and in vivo studies have shown the prebiotic properties of OβG and its capacity to enhance SCFAs production, especially butyrate and propionate [15,41,42]. Notably, the SCFAs, particularly butyrate, are recognised for their pro-apoptotic and anti-proliferative effects on colorectal cancer cells [43]. These fatty acids induce apoptosis in colorectal cancer cells by modulating the expression of caspase-3 [44]. In addition, butyric acid has been shown to reduce the proliferation of colorectal cancer cells while, conversely, increasing the proliferation of non-cancerous colon cells [45]. Moreover, the anti-cancer properties of SCFAs are closely associated with their immunomodulatory properties. Both butyrate and propionate can stimulate T cells, leading to the production of key cytokines such as IFN-γ and TNF-α, which in turn induce apoptosis in cancer cells and inhibit their growth [46].

In our study, induction of carcinogenesis by intraperitoneal administration of azoxymethane resulted in a significant decrease in the expression of PARP-1 in the colorectal mucosa and full-length PARP-1 in the colorectal wall, which is an important enzyme involved in DNA damage repair. PARP-1 deficiency with increased DNA damage induced by exposure to a carcinogen, without increased apoptosis, is associated with an increased risk of cancer cell formation and survival. Therefore, the effect of counteracting the reduction in PARP-1 expression by OβGl, as was demonstrated in our study, appears to have a beneficial effect related to enhanced DNA repair. Importantly, OβGl did not induce overexpression of PARP-1, despite the level of expression being similar to the control groups. It appears that PARP-1 overexpression could promote the survival of cells with extensive DNA damage, which would be associated with a risk of neoplastic transformation [47]. Furthermore, as other studies show, PARP-1 may protect against colorectal cancer induction by initiating DNA repair, but on the other hand, it may promote inflammation-driven colorectal cancer progression through inflammation via the innate immune response and promote colorectal tumour growth through activation of the IL6-STAT3-cyclin D1 axis [21]. It is therefore important to maintain PARP-1 expression at an appropriate level. Such an effect can be exerted by OβGl, as demonstrated in our study.

Intriguingly, we found no effects of OβGl on the markers of apoptosis and autophagy in the normal colorectum of rats (no CRC induction), which proves the safe usage of these polysaccharides. The safety of OβG is also confirmed by the results of our previous study on the effects of OβG of different molar masses on inflammation in a model of Crohn's disease. The results showed no or very slight effect of OβGs on several different parameters such as the levels of pro- and anti-inflammatory cytokines, the expression of chemokines and their receptors, and the expression of apoptosis and autophagy markers in the colon of rats without induced inflammation. In contrast, the same results showed strong beneficial properties of high and low-molar-mass OβG associated with suppression of induced inflammation including the modulatory effects on apoptosis and autophagy in colonocytes [10,12,16,48]. OβG inhibited excessive apoptosis and had a stimulatory effect on autophagy in colon inflammation, with a stronger effect of low-molar-mass oat beta-glucan. Three weeks after the induction of inflammation, aberrant crypts also began to appear on the inflamed colon wall (Supplementary Fig. 4), proving initial pro-cancerous changes are driven by inflammation [16]. In summary, these results demonstrate the strong immunomodulatory properties of beta-glucans from oats, particularly the low-molar-mass fraction.

5. Conclusions

Our study demonstrated, for the first time, that low-molar-mass oat beta-glucan consumption as a feed supplement significantly stimulated autophagy and apoptosis processes in the colorectal mucosa during the early stage of the carcinogenesis process by increasing the expression of LC3B, LC3B-II, caspase-3 and cleaved caspase-3. The dose-dependent and more substantial effect was exerted by the 3 % addition of OβGl to the feed. Furthermore, the addition of 3 % OβGl to the feed probably

stimulated apoptosis via the extrinsic pathway by not influencing BAX expression and the BAX/BCL-2 ratio. In contrast, the addition of 1 % OβGl did not modulate the expression of LC3B and cleaved-caspase-3. Instead, it increased the BAX/BCL-2 ratio, indicating a stimulatory effect on the intrinsic apoptotic pathway. OβGl counteracted the reduction in PARP-1 expression caused by CRC induction, demonstrating a stimulatory effect on DNA repair. It is also important to note that the modulatory effect of OβGl on the activity of autophagy and apoptosis was only observed in colorectum altered by cancer development, and there was no such effect in healthy tissue. These properties suggest that OβGl consumption is safe.

5.1. Limitation

The limiting factor for the results of our study is the use of a short experimental period – minimal to obtain an early stage of carcinogenesis using azoxymethane. A more extended experimental period, e.g. 12–16 weeks, would have resulted in a stronger effect in cancer lesions in the colorectum and a more pronounced effect of low-molar-mass oat beta-glucan would be demonstrated.

Supplementary data to this article can be found online at https://doi.org/10.1016/j.ijbiomac.2023.127832.

CRediT authorship contribution statement

Łukasz Kopiasz: Investigation, Data Curation, Formal analysis, Methodology, Visualization, Writing - original draft. **Katarzyna Dziendzikowska**: Investigation, Writing - review & editing. **Michał Oczkowski**: Investigation, Writing - review & editing. **Joanna Harasym**: Resources, Writing - review & editing. **Joanna Gromadzka-Ostrowska**: Funding acquisition, Writing - review & editing. All authors have read and agreed to the published version of the manuscript.

Declaration of competing interest

The authors declare that they have no known competing financial interests or personal relationships that could have appeared to influence the work reported in this paper.

Data availability

Data will be made available on request.

Acknowledgments

We would like to acknowledge Alicja Majewska from Institute of Veterinary Medicine, Warsaw University of Life Sciences (IVM-WULS) for support with the PCR analyses and Małgorzata Gajewska from IVM-WULS for advice on Western blot analysis.

Ethics approval

The animal experiment was conducted after the approval of the 2nd Local Ethical Committee in Warsaw (Resolution No. WAW2/040/2019) in accordance with the EU Directive 2010/63/EU for animal experiments and Polish law and 3R rules (*Replacement*, *Reduction and Refinement*).

Funding

The study was financed by the National Science Centre, Poland through grant number 2018/29/B/NZ9/01060.

References

[1] A. Venugopal, J.M. Carethers, Epidemiology and biology of early onset colorectal cancer, EXCLI J. 21 (2022) 162–182, https://doi.org/10.17179/excli2021-4456.
[2] World Health Organization, Colorectal cancer, Int. Agency Res. Cancer (2020) 1–2. https://gco.iarc.fr/today/data/factsheets/cancers/10_8_9-Colorectum-fact-sheet.pdf.
[3] M.S. Hossain, H. Karuniawati, A.A. Jairoun, Z. Urbi, D.J. Ooi, A. John, Y.C. Lim, K. M.K. Kibria, A.K.M. Mohiuddin, L.C. Ming, K.W. Goh, M.A. Hadi, Colorectal cancer: a review of carcinogenesis, global epidemiology, current challenges, risk factors, preventive and treatment strategies, Cancers (Basel). 14 (2022) 1732, https://doi.org/10.3390/cancers14071732.
[4] L. Sushytskyi, A. Synytsya, J. Čopíková, P. Lukáč, L. Rajsiglová, P. Tenti, L. E. Vannucci, Perspectives in the application of high, medium, and low molecular weight oat β-D-glucans in dietary nutrition and food technology — a short overwiew, Foods 12 (2023) 1121, https://doi.org/10.3390/foods12061121.
[5] R.L. Shen, Z. Wang, J.L. Dong, Q. Sen Xiang, Y.Q. Liu, Effects of oat soluble and insoluble β-glucan on 1,2-dimethylhydrazine-induced early colon carcinogenesis in mice, Food Agric. Immunol. 27 (2016) 657–666, https://doi.org/10.1080/09540105.2016.1148664.
[6] A. Choromańska, J. Kulbacka, N. Rembiałkowska, J. Piłat, R. Olędzki, J. Harasym, J. Saczko, Anticancer properties of low molecular weight oat beta-glucan - an in vitro study, Int. J. Biol. Macromol. 80 (2015) 23–28, https://doi.org/10.1016/j.ijbiomac.2015.05.035.
[7] A. Choromańska, J. Kulbacka, J. Harasym, R. Oledzki, A. Szewczyk, J. Saczko, High- and low-molecular weight oat beta-glucan reveals antitumor activity in human epithelial lung cancer, Pathol. Oncol. Res. 24 (2018) 583–592, https://doi.org/10.1007/s12253-017-0278-3.
[8] A. Parzonko, M. Makarewicz-Wujec, E. Jaszewska, J. Harasym, M. Kozłowska-Wojciechowska, Pro-apoptotic properties of (1,3)(1,4)-β-d-glucan from Avena sativa on human melanoma HTB-140 cells in vitro, Int. J. Biol. Macromol. 72 (2015) 757–763, https://doi.org/10.1016/j.ijbiomac.2014.09.033.
[9] A. Shah, M. Ahmad, B.A. Ashwar, A. Gani, F.A. Masoodi, I.A. Wani, S.M. Wani, A. Gani, Effect of γ-irradiation on structure and nutraceutical potential of β-d-glucan from barley (Hordeum vulgare), Int. J. Biol. Macromol. 72 (2015) 1168–1175, https://doi.org/10.1016/j.ijbiomac.2014.08.056.
[10] E. Żyła, K. Dziendzikowska, M. Gajewska, J. Wilczak, J. Harasym, J. Gromadzka-ostrowska, Beneficial effects of oat beta-glucan dietary supplementation in colitis depend on its molecular weight, Molecules 24 (2019) 3591, https://doi.org/10.3390/molecules24193591.
[11] D. Suchecka, K. Błaszczyk, J. Harasym, S. Gudej, J. Wilczak, J. Gromadzka-Ostrowska, Impact of purified oat 1-3, 1-4-β-d-glucan of different molecular weight on alleviation of inflammation parameters during gastritis, J. Funct. Foods 28 (2017) 11–18, https://doi.org/10.1016/j.jff.2016.10.028.
[12] E. Żyła, K. Dziendzikowska, D. Kamola, J. Wilczak, R. Sapierzyński, J. Harasym, J. Gromadzka-Ostrowska, Anti-inflammatory activity of oat beta-glucans in a crohn's disease model: time-and molar mass-dependent effects, Int. J. Mol. Sci. 22 (2021), https://doi.org/10.3390/ijms22094485.
[13] Ł. Kopiasz, K. Dziendzikowska, M. Gajewska, J. Wilczak, J. Harasym, E. Żyła, D. Kamola, M. Oczkowski, T. Królikowski, J. Gromadzka-Ostrowska, Time-dependent indirect antioxidative effects of oat beta-glucans on peripheral blood parameters in the animal model of colon inflammation, Antioxidants 9 (2020) 375, https://doi.org/10.3390/antiox9050375.
[14] K. Błaszczyk, J. Wilczak, J. Harasym, S. Gudej, D. Suchecka, T. Królikowski, E. Lange, J. Gromadzka-Ostrowska, Impact of low and high molecular weight oat beta-glucan on oxidative stress and antioxidant defense in spleen of rats with LPS induced enteritis, Food Hydrocoll. 51 (2015) 272–280, https://doi.org/10.1016/j.foodhyd.2015.05.025.
[15] J. Wilczak, K. Błaszczyk, D. Kamola, M. Gajewska, J.P. Harasym, M. Jałosińska, S. Gudej, D. Suchecka, M. Oczkowski, J. Gromadzka-Ostrowska, The effect of low or high molecular weight oat beta-glucans on the inflammatory and oxidative stress status in the colon of rats with LPS-induced enteritis, Food Funct. 6 (2015) 590–603, https://doi.org/10.1039/c4fo00638k.
[16] Ł. Kopiasz, K. Dziendzikowska, M. Gajewska, M. Oczkowski, K. Majchrzak-Kuligowska, T. Królikowski, J. Gromadzka-ostrowska, Effects of dietary oat beta-glucans on colon apoptosis and autophagy through tlrs and dectin-1 signaling pathways—Crohn's disease model study, Nutrients 13 (2021) 321, https://doi.org/10.3390/nu13020321.
[17] A. Letai, Apoptosis and cancer, Annu. Rev. Cancer Biol. 1 (2017) 275–294, https://doi.org/10.1146/annurev-cancerbio-050216-121933.
[18] A. Boice, L. Bouchier-Hayes, Targeting apoptotic caspases in cancer, Biochim. Biophys. Acta, Mol. Cell Res. 1867 (2020), 118688, https://doi.org/10.1016/j.bbamcr.2020.118688.
[19] D.R. Green, F. Llambi, Cell death signaling, Cold Spring Harb. Perspect. Biol. 7 (2015), a006080, https://doi.org/10.1101/cshperspect.a006080.
[20] B.A. Carneiro, W.S. El-Deiry, Targeting apoptosis in cancer therapy, Nat. Rev. Clin. Oncol. 17 (2020) 395–417, https://doi.org/10.1038/s41571-020-0341-y.
[21] B. Dörsam, N. Seiwert, S. Foersch, S. Stroh, G. Nagel, D. Begaliew, E. Diehl, A. Kraus, M. McKeague, V. Minneker, V. Roukos, S. Reißig, A. Waisman, M. Moehler, A. Stier, A. Mangerich, F. Dantzer, B. Kaina, J. Fahrer, PARP-1 protects against colorectal tumor induction, but promotes inflammation-driven colorectal tumor progression, Proc. Natl. Acad. Sci. U. S. A. 115 (2018) E4061–E4070, https://doi.org/10.1073/pnas.1712345115.
[22] K.K. Patel, T.S. Stappenbeck, Autophagy and intestinal homeostasis, Annu. Rev. Physiol. 75 (2013) 241–262, https://doi.org/10.1146/annurev-physiol-030212-183658.Autophagy.

[23] S. Saha, D.P. Panigrahi, S. Patil, S.K. Bhutia, Autophagy in health and disease: a comprehensive review, Biomed. Pharmacother. 104 (2018) 485–495, https://doi.org/10.1016/j.biopha.2018.05.007.
[24] M.I. Koukourakis, D. Kalamida, A. Giatromanolaki, C.E. Zois, E. Sivridis, S. Pouliliou, A. Mitrakas, K.C. Gatter, A.L. Harris, Autophagosome proteins LC3A, LC3B and LC3C have distinct subcellular distribution kinetics and expression in cancer cell lines, PLoS One 10 (2015), e0137675, https://doi.org/10.1371/journal.pone.0137675.
[25] H.D. Xu, Z.H. Qin, Beclin 1, Bcl-2 and autophagy, in: Z.H. Qin (Ed.), Autophagy Biol. Dis. Adv. Exp. Med. Biol, Springer Singapore, 2019, pp. 109–126, https://doi.org/10.1007/978-981-15-0602-4_5.
[26] S. Kaur, H. Changotra, The beclin 1 interactome: modification and roles in the pathology of autophagy-related disorders, Biochimie 175 (2020) 34–49, https://doi.org/10.1016/j.biochi.2020.04.025.
[27] M. Perše, A. Cerar, Morphological and molecular alterations in 1,2 dimethylhydrazine and azoxymethane induced colon carcinogenesis in rats, J. Biomed. Biotechnol. 2011 (2011), https://doi.org/10.1155/2011/473964.
[28] J. Harasym, E. Żyła, K. Dziendzikowska, J. Gromadzka-Ostrowska, Proteinaceous residue removal from oat β-glucan extracts obtained by alkaline water extraction, Molecules 24 (2019) 1729, https://doi.org/10.3390/molecules24091729.
[29] J. Harasym, D. Suchecka, J. Gromadzka-Ostrowska, Effect of size reduction by freeze-milling on processing properties of beta-glucan oat bran, J. Cereal Sci. 61 (2015) 119–125, https://doi.org/10.1016/j.jcs.2014.10.010.
[30] P.G. Reeves, F.H. Nielsen, G.C. Fahey, AIN-93 purified diets for laboratory rodents: final report of the American Institute of Nutrition ad hoc writing committee on the reformulation of the AIN-76A rodent diet, J. Nutr. 123 (1993) 1939–1951, https://doi.org/10.1093/jn/123.11.1939.
[31] J.H.A.J. Curfs, A. Chwalibog, B.S. Savenije, M. Ritskes-Hoitinga, Nutrient requirements, experimental design, and feeding schedules in animal experimentation, in: J. Hau, S.J. Schapiro (Eds.), Handb. Lab. Anim. Sci. Vol. 1, Essent. Princ. Pract, Third edit., Taylor & Francis Group, 2011, pp. 307–342.
[32] J. Long, Q. He, Y. Yin, X. Lei, Z. Li, W. Zhu, The effect of miRNA and autophagy on colorectal cancer, Cell Prolif. 53 (2020), e12900, https://doi.org/10.1111/cpr.12900.
[33] H. Zhou, M. Yuan, Q. Yu, X. Zhou, W. Min, D. Gao, Autophagy regulation and its role in gastric cancer and colorectal cancer, Cancer Biomark. 17 (2016) 1–10, https://doi.org/10.3233/CBM-160613.
[34] M. Xu, F. Ling, J. Li, Y. Chen, S. Li, Y. Cheng, L. Zhu, Oat beta-glucan reduces colitis by promoting autophagy flux in intestinal epithelial cells via EPHB6-TFEB axis, Front. Pharmacol. 14 (2023), e1189229, https://doi.org/10.3389/fphar.2023.1189229.
[35] S. Das, N. Shukla, S.S. Singh, S. Kushwaha, R. Shrivastava, Mechanism of interaction between autophagy and apoptosis in cancer, Apoptosis 26 (2021) 512–533, https://doi.org/10.1007/s10495-021-01687-9.
[36] M.L. Clapper, W.C.L. Chang, H.S. Cooper, Dysplastic aberrant crypt foci: biomarkers of early colorectal neoplasia and response to preventive intervention, Cancer Prev. Res. 13 (2020) 229–239, https://doi.org/10.1158/1940-6207.CAPR-19-0316.
[37] R. Jan, G.-S. Chaudhry, Understanding apoptosis and apoptotic pathways targed cancer therapeutics, Adv. Pharm. Bull. 9 (2019) 205–218, https://doi.org/10.15171/apb.2019.024.
[38] M. Zhang, L. Chun, V. Sandoval, H. Graor, J. Myers, J. Nthale, P. Rauhe, Z. Senders, K. Choong, A.Y. Huang, J. Kim, Systemic administration of β-glucan of 200 kDa modulates melanoma microenvironment and suppresses metastatic cancer, Oncoimmunology 7 (2018), e1387347, https://doi.org/10.1080/2162402X.2017.1387347.
[39] J. Gao, M. Senthil, B. Ren, J. Yan, Q. Xing, J. Yu, L. Zhang, J.H. Yim, IRF-1 transcriptionally upregulates PUMA, which mediates the mitochondrial apoptotic pathway in IRF-1-induced apoptosis in cancer cells, Cell Death Differ. 17 (2010) 699–709, https://doi.org/10.1038/cdd.2009.156.
[40] H. Wang, Y. Huang, J. He, L. Zhong, Y. Zhao, Dual roles of granzyme B, Scand. J. Immunol. 94 (2021), e13086, https://doi.org/10.1111/sji.13086.
[41] J. Bai, T. Li, W. Zhang, M. Fan, H. Qian, Y. Li, L. Wang, Systematic assessment of oat β-glucan catabolism during in vitro digestion and fermentation, Food Chem. 348 (2021), 129116, https://doi.org/10.1016/j.foodchem.2021.129116.
[42] J. Bai, J. Zhao, W. Al-Ansi, J. Wang, L. Xue, J. Liu, Y. Wang, M. Fan, H. Qian, Y. Li, L. Wang, Oat β-glucan alleviates DSS-induced colitis via regulating gut microbiota metabolism in mice, Food Funct. 12 (2021) 8976–8993, https://doi.org/10.1039/d1fo01446c.
[43] R. Mirzaei, A. Afaghi, S. Babakhani, M.R. Sohrabi, S.R. Hosseini-Fard, K. Babolhavaeji, S. Khani Ali Akbari, R. Yousefimashouf, S. Karampoor, Role of microbiota-derived short-chain fatty acids in cancer development and prevention, Biomed. Pharmacother. 139 (2021), 111619, https://doi.org/10.1016/j.biopha.2021.111619.
[44] L. Pattayil, H.-T. Balakrishnan Saraswathi, In vitro evaluation of apoptotic induction of butyric acid derivatives in colorectal carcinoma cells, Anticancer Res. 39 (2019) 3795–3801, https://doi.org/10.21873/anticanres.13528.
[45] A. Han, N. Bennett, B. Ahmed, J. Whelan, D.R. Donohoe, Butyrate decreases its own oxidation in colorectal cancer cells through inhibition of histone deacetylases, Oncotarget 9 (2018) 27280–27292, https://doi.org/10.18632/oncotarget.25546.
[46] G.H. Al-Qadami, K.R. Secombe, C.B. Subramaniam, H.R. Wardill, J.M. Bowen, Gut microbiota-derived short-chain fatty acids: impact on cancer treatment response and toxicities, Microorganisms 10 (2022) 2048, https://doi.org/10.3390/microorganisms10102048.
[47] S. Pazzaglia, C. Pioli, Multifaceted role of parp-1 in dna repair and inflammation: pathological and therapeutic implications in cancer and non-cancer diseases, Cells 9 (2020) 41, https://doi.org/10.3390/cells9010041.
[48] Ł. Kopiasz, K. Dziendzikowska, J. Gromadzka-ostrowska, Colon expression of chemokines and their receptors depending on the stage of colitis and oat beta-glucan dietary intervention—Crohn's disease model study, Int. J. Mol. Sci. 23 (2022) 1406, https://doi.org/10.3390/ijms23031406.

Wyrażam zgodę na udostępnianie mojej pracy w czytelniach Biblioteki SGGW.

Łukasz Kamiński
.....
(czytelny podpis autora)